

UNIVERSIDAD SAN FRANCISCO DE QUITO USFQ

Colegio de Ciencias e Ingenierías

**Effectivity of non-modified cellulose for heavy metal removal
from water**

Gabriela Isabel Vivanco Jaramillo

Ingeniería Química

Trabajo de fin de carrera presentado como requisito
para la obtención del título de
Ingeniera Química

Quito, 20 de diciembre de 2022

UNIVERSIDAD SAN FRANCISCO DE QUITO USFQ

Colegio de Ciencias e Ingenierías

HOJA DE CALIFICACIÓN DE TRABAJO DE FIN DE CARRERA

Effectivity of non-modified cellulose for heavy metal removal from water

Gabriela Isabel Vivanco Jaramillo

Nombre del profesor, Título académico

Frank Alexis, Ph.D.

Nombre del profesor, Título académico

David Egas, Ph.D.

Quito, 20 de diciembre de 2022

© DERECHOS DE AUTOR

Por medio del presente documento certifico que he leído todas las Políticas y Manuales de la Universidad San Francisco de Quito USFQ, incluyendo la Política de Propiedad Intelectual USFQ, y estoy de acuerdo con su contenido, por lo que los derechos de propiedad intelectual del presente trabajo quedan sujetos a lo dispuesto en esas Políticas.

Asimismo, autorizo a la USFQ para que realice la digitalización y publicación de este trabajo en el repositorio virtual, de conformidad a lo dispuesto en la Ley Orgánica de Educación Superior del Ecuador.

Nombres y apellidos: Gabriela Isabel Vivanco Jaramillo

Código: 00205895

Cédula de identidad: 1722254537

Lugar y fecha: Quito, 20 de diciembre de 2022

ACLARACIÓN PARA PUBLICACIÓN

Nota: El presente trabajo, en su totalidad o cualquiera de sus partes, no debe ser considerado como una publicación, incluso a pesar de estar disponible sin restricciones a través de un repositorio institucional. Esta declaración se alinea con las prácticas y recomendaciones presentadas por el Committee on Publication Ethics COPE descritas por Barbour et al. (2017) Discussion document on best practice for issues around theses publishing, disponible en <http://bit.ly/COPETHeses>.

UNPUBLISHED DOCUMENT

Note: The following capstone project is available through Universidad San Francisco de Quito USFQ institutional repository. Nonetheless, this project – in whole or in part – should not be considered a publication. This statement follows the recommendations presented by the Committee on Publication Ethics COPE described by Barbour et al. (2017) Discussion document on best practice for issues around theses publishing available on <http://bit.ly/COPETHeses>.

RESUMEN

En la presente investigación se investigó el efecto de la concentración inicial e identidad de metales pesados, y dosis de adsorbente en la eliminación de metales pesados del agua. Ocho materiales celulósicos se eligieron para estudiar la remoción de iones de Cu, Cd y Pb de soluciones controladas con concentraciones entre 1 y 100 ppm. Se realizó un análisis de composición de los materiales extraídos utilizando las técnicas de FTIR y TGA. Estos análisis mostraron que las muestras utilizadas son de composición compleja, con un porcentaje en peso significativo de hemicelulosa. Los ensayos de adsorción por lotes se realizaron al exponer cada una de las soluciones de iones metálicos controladas a 3 dosis de adsorbente. Las concentraciones de los iones metálicos presentes remanente fueron analizadas por espectroscopía de absorción atómica. Los materiales Ad y N2 mostraron el menor porcentaje de metal remanente en solución, lo cual fue atribuido a su composición compleja. Los resultados del estudio de los modelos teóricos se vieron afectado negativamente por la variabilidad de los datos obtenidos. Esta variabilidad se atribuyó al método de detección, y puede contrarrestarse con la realización por triplicado de los ensayos para la obtención de datos estadísticamente relevantes.

Palabras clave: metales pesados, remediación de agua, cobre, cadmio, plomo, celulosa, bioadsorción.

ABSTRACT

On this project, the effect of initial metal-ion concentration and identity, and adsorbent dose on heavy metal removal from water was assessed. Eight cellulosic materials were chosen as adsorbents to study removal of Cu, Cd and Pb ions from control solutions ranging from 1 to 100 ppm. Composition analysis of the materials was done by FTIR and TGA analysis, concluding that extracted samples had complex compositions with significant presence of hemicellulose. Batch adsorption essays were performed by exposing each metal control solutions to 3 concentrations of adsorbent. Analysis of metal-ion concentration remaining in solution after the essays was done by atomic absorption spectroscopy. Materials Ad and N2 showed the lowest percentage of metal remaining in solution for every metal. Further analysis concluded that the complex composition of both materials benefited adsorption effectiveness. Isotherm theoretical models were greatly affected by data variability, attributed to the detection method, that could be improved by performing the essays several times and drawing statistically significant data.

Key words: heavy metal, water remediation, copper, cadmium, lead, cellulose, biosorption.

TABLE OF CONTENTS

1. Introduction.....	13
2. Methodology.....	16
2.1 Materials	16
2.1.1 Cellulose	16
2.1.2 Reagents.....	16
2.2 Extraction and analysis of cellulose.....	16
2.2.1 Extraction method.....	16
2.2.2 FTIR.....	17
2.2.3 TGA	17
2.3 Adsorption essays	18
2.3.1 Standard preparation	18
2.3.2 Batch adsorption essays	18
2.4 Atomic absorption spectroscopy (AAS)	19
2.5 Adsorption Isotherm models.....	19
3. Results and discussions.....	21
3.1 Composition analysis of the materials	21
3.2 Changes in the samples after batch adsorption essays.....	24
3.3 Adsorption Essays.....	25
3.4 Isotherm studies	30
3.4.1 Copper.....	30

3.4.2 Lead.....	31
3.4.3 Cadmium.....	32
4. Conclusions and Recommendations	33
5. References.....	35
6. Annexes.....	38
Annex A: Thermal curves (TGA) and their respective derivatives	38
Annex B: FTIR spectra before and after adsorption	42
Annex C: Curve fitting graphs to isotherm models	46
Annex D: Summary of Curve fittings to isotherm models	59

TABLE INDEX

Table 1. Initial metal-ion solutions prepared for adsorption essays	18
Table 2. Flame atomic adsorption concentration ranges	19
Table 3. Temperature of maximum decomposition for main components on the original materials.....	22
Table 4. Percentage of metal remaining in solution from initial concentration of 70 ppm	30
Table 5. Summary of model fitting results	31
Table 6. Summary of model fitting results	31
Table 7. Summary of model fitting results	32
Table 8. Summary of curve fittings for copper data	59
Table 9. Summary of curve fittings for lead data	60
Table 10. Summary of curve fittings for cadmium data	61

FIGURE INDEX

Figure 1. FTIR spectra of extracted materials and commercial cellulose.....	21
Figure 2. FTIR spectra of material N2 after adsorption essays	25
Figure 3. Percentage of metal remaining in solution from initial concentration of 50 ppm using adsorbent at a concentration of 5 mg/mL.	26
Figure 4. Percentage of metal remaining in solution from initial concentration of 10 ppm using adsorbent at a concentration of 5 mg/mL.	27
Figure 5. TGA curves for material N2.....	38
Figure 6. TGA curves for material G.....	38
Figure 7. TGA curves for material C4.....	39
Figure 8. TGA curves for material C1	39
Figure 9. TGA curves for material C.....	40
Figure 10. TGA curves for material B1	40
Figure 11. TGA curves for material Af	41
Figure 12. TGA curves for material Ad.....	41
Figure 13. FTIR spectra for material N2	42
Figure 14. FTIR spectra for material G	42
Figure 15. FTIR spectra for material C4.....	43
Figure 16. FTIR spectra for material C1.....	43
Figure 17. FTIR spectra for material C.....	44
Figure 18. FTIR spectra for material B1.....	44
Figure 19. FTIR spectra for material Af.....	45
Figure 20. FTIR spectra for material Ad	45

Figure 21. Curve fittings for material C1 with cellulose concentration of a) 1mg/mL b) 3 mg/mL and c) 5 mg/mL	46
Figure 22. Curve fittings for material C4 with cellulose concentration of a) 1mg/mL b) 3 mg/mL and c) 5 mg/mL	47
Figure 23. Curve fittings for material B1 with cellulose concentration of a) 1mg/mL b) 3 mg/mL and c) 5 mg/mL	47
Figure 24. Curve fittings for material Ad with cellulose concentration of a) 1mg/mL b) 3 mg/mL and c) 5 mg/mL	48
Figure 25. Curve fittings for material N2 with cellulose concentration of a) 1mg/mL b) 3 mg/mL and c) 5 mg/mL	48
Figure 26. Curve fittings for material C with cellulose concentration of a) 1mg/mL b) 3 mg/mL and c) 5 mg/mL.....	49
Figure 27. Curve fittings for material G with cellulose concentration of a) 1mg/mL b) 3 mg/mL and c) 5 mg/mL.....	49
Figure 28. Curve fittings for material Af with cellulose concentration of a) 1mg/mL b) 3 mg/mL and c) 5 mg/mL.....	50
Figure 29. Curve fittings for material B1 with cellulose concentration of a) 1mg/mL b) 3 mg/mL and c) 5 mg/mL	50
Figure 30. Curve fittings for material N2 with cellulose concentration of a) 1mg/mL b) 3 mg/mL and c) 5 mg/mL	51
Figure 31. Curve fittings for material G with cellulose concentration of a) 1mg/mL b) 3 mg/mL and c) 5 mg/mL.....	51
Figure 32. Curve fittings for material Ad with cellulose concentration of a) 1mg/mL b) 3 mg/mL and c) 5 mg/mL	52

Figure 33. Curve fittings for material Af with cellulose concentration of a) 1mg/mL b) 3 mg/mL and c) 5 mg/mL.....	52
Figure 34. Curve fittings for material C with cellulose concentration of a) 1 mg/mL b) 3 mg/mL and c) 5 mg/mL.....	53
Figure 35. Curve fittings for material C1 with cellulose concentration of a) 1mg/mL b) 3 mg/mL and c) 5 mg/mL.....	53
Figure 36. Curve fittings for material C4 with cellulose concentration of a) 1mg/mL b) 3 mg/mL and c) 5 mg/mL.....	54
Figure 37. Curve fittings for material G with cellulose concentration of a) 1mg/mL b) 3 mg/mL and c) 5 mg/mL.....	54
Figure 38. Curve fittings for material B1 with cellulose concentration of a) 1mg/mL b) 3 mg/mL and c) 5 mg/mL.....	55
Figure 39. Curve fittings for material N2 with cellulose concentration of a) 1mg/mL b) 3 mg/mL and c) 5 mg/mL.....	55
Figure 40. Curve fittings for material C with cellulose concentration of a) 1mg/mL b) 3 mg/mL and c) 5 mg/mL.....	56
Figure 41. Curve fittings for material Ad with cellulose concentration of a) 1mg/mL b) 3 mg/mL and c) 5 mg/mL.....	56
Figure 42. Curve fittings for material C1 with cellulose concentration of a) 1mg/mL b) 3 mg/mL and c) 5 mg/mL.....	57
Figure 43. Curve fittings for material C4 with cellulose concentration of a) 1mg/mL b) 3 mg/mL and c) 5 mg/mL.....	57
Figure 44. Curve fittings for material Af with cellulose concentration of a) 1 mg/mL b) 3 mg/mL and c) 5 mg/mL.....	58

1. INTRODUCTION

Heavy metals are atoms of high atomic weight and density that, although they can be found in natural occurring settings, high exposure to them is toxic for human beings, animals, and plants. Copper, cadmium, and lead are among the most frequent heavy metal pollutants [1]. Health issues associated to exposure to them include impediments to neurodevelopment, respiratory and reproductive conditions, and effects on the liver and kidneys [2], [3]. These metals enter the environment mainly because of mining activities, refining, and smelting, but are also present in effluents of plastic and pigment production [3], [4]. Once heavy metals enter the environment, they can climb the food chain up to human food sources, or they can stay dissolved in water and emerge in house water faucets. This last scenario is the main concern for the present research, especially considering that the prevention of human intake of heavy metals from water sources is an issue yet to be addressed in Ecuador.

Exposure to lead is increasing in some parts of the world, particularly in developing countries, where poverty, malnutrition, and lack of education make pollution-derived health problems worse. Olivero-Verbel et. al. show a compilation of data regarding lead and mercury exposure and poisoning in Latin America [5]. However, data was only available for Brazil, Argentina, Uruguay, Colombia, and Mexico. This portrays a concerning problem: heavy metal detection and regulation are lacking in the region. In Ecuador, water treatment facilities do not have means to detect heavy metals, let alone ways to eliminate them. Increasing water pollution in the Amazonian region, especially in the Sucumbíos and Orellana provinces, has been linked to mining and intensive toxic agrochemical use, causing extensive damage to nearby populations [6]. With this in mind, developing ways to eliminate heavy metals from possible sources of human consumption is necessary.

Conventional methods can involve complex and expensive processes that, considering limited space and technological capacity of Ecuadorian treatment facilities, are not implementable in the country. Conventional heavy metal removing methods include adsorption-, membrane-, chemical- and electric- treatments. Some of the challenges regarding these techniques are low removal ability of heavy metals, formation of toxic sludge, fouling, high energy requirements, large dosage of reactants, automaticity, need of more research on stability and difficulty on large-scale application [7]. Although the presented techniques are adaptable regarding materials and chemicals used, adsorption continues to be the most attention-grabbing alternative. In this sense, biosorption has emerged as a trend in acquiring efficient and cost-effective methods of heavy metal removal from water.

Adsorption is one of the main focuses of recent studies on heavy metal removal, which include carbon -, chitosan- and mineral-based adsorbents, and biosorbents [7]. Adsorption is the physical adherence or bonding of ions and molecules onto the surface of another molecule, in a two-dimensional surface [8]. The greatest disadvantage of this process is the desorption of the adsorbate from the adsorbent after the procedure. However, once the adsorbent material is regenerated, it can be reutilized or destined to other activities. And, based on the regeneration methods, adsorption is considered as an environmentally acceptable method [9]. Carbon- and chitosan-based adsorbents require surface modification for heavy metal removal and improvement on physical properties. Mineral and magnetic adsorbents are reliant on pH and other conditions for optimal adsorption capacity. Additionally, an important consideration in water remediation through adsorption is that the materials are not possible pollutants after use.

Considering Ecuador's high fruit and vegetable production and waste, cellulose appears to be an advantageous option for biosorption. Cellulose is a readily available material that as it can be extracted from a variety of sources. Also, the viability of biomass, from agricultural and

food waste, for different purposes is of big research interest, especially considering the waste is often high in cellulose content [10]. Banana and orange peels, peanut shells, wood bark, sugarcane bagasse, rice husk and mango seeds, have been studied as heavy metal removing biosorbents [10]–[13]. In Ecuador, heavy metal removal has been addressed through yeast species and microalgae, for cellulose use of heavy metal remediation is new in the country [14], [15]. Also, since studies in cellulose use for heavy metal adsorption have focused mainly on modified cellulosic materials, inquiring on the natural counterpart is innovative.

To reduce human intake of heavy metals from water, the main purpose of this work is to study the effectivity of non-modified cellulose obtained from fruits cultivated in Ecuador for the elimination of heavy metals from water sources. For this, physicochemical properties of eight non-modified celluloses were examined to determine the properties of these materials that could affect heavy metal adsorption. This examination was conducted through analytical methods, such as FTIR and TGA. Following this, batch adsorption essays were done by mixing heavy metal solutions with the extracted materials and analyzing the liquid phase to identify the cellulose with the highest adsorption capacity. The following sections plan to expand on the execution, examination, and evaluation of employing cellulose for Cu, Pb and Cd adsorption.

2. METHODOLOGY

2.1 Materials

2.1.1 Cellulose

The election of the celluloses used in this research was based on preliminary results obtained by Caicho, J. on the possibility of using fruit/vegetable waste as adsorbent materials [16]. Four of these celluloses (N2, B1, G, Ad) were selected to be compared on their adsorption effectiveness with four control materials (C, C1, Af, C4). The samples were extracted from products cultivated in Ecuador that were acquired from local markets: “Mercado Municipal de La Kennedy” and “Micro Mercado Li Frutti”. All the sources are free of restrictions regarding their use, meaning that there is no environmental, social, or economic control regarding their use and harvest. The control materials are commercial celluloses provided by Sigma-Aldrich and Alfa Aesar and waste from a plant found in Ecuador. Also, a commercial water filter, YakuPura, will also be tested for heavy metal removal.

2.1.2 Reagents

Regarding the adsorption essays, the studied solutions were prepared from a standard 1000 ppm solution of each metal provided by AccuStandard, a manufacturer of certified reference materials. These solutions were also used for the generation of the respective calibration curves.

2.2 Extraction and analysis of cellulose

2.2.1 Extraction method

Cellulose extraction was made from 4 different products cultivated in Ecuador with potential for heavy metal adsorption following the methods of Bravo et al. and Morán et al., with modifications [17], [18]. These materials were: Ad, B1, G and N2.

Pulp from the sources was generated and then subjected to an acid/base treatment. The extracted material was bleached and washed several times in order to remove residual reagents from the process. Finally, the obtained substance was dried by lyophilization. Once the cellulose dried, the characterization and essays were performed.

2.2.2 FTIR

Fourier-transform infrared spectroscopy is method of characterization that provides an infrared spectrum of emission of the solid studied, the cellulose in this case [19]. The main findings provided by this method include identification of functional groups and relevant interactions within the molecule. This analysis was done for the original extracted celluloses as well as for the material after adsorption using the equipment Cary 630 FTIR spectrometer from Agilent Technologies. Also, this method is rapid and not destructive for the characterization of the biomass compound.

2.2.3 TGA

Thermogravimetric analysis measures change in the weight of a sample, in a defined atmosphere, as a function of temperature [5]. When coupled with infrared techniques, TGA can be used to determine chemical identification and composition. The progression of the analysis involves weight losses with increasing temperatures. These weight losses happen at specific temperatures that can be correlated to certain species, hence, providing an insight on the composition of the sample. Thermogravimetric analysis was done on the original extracted and control materials as to corroborate the presence of cellulose. The tests were programmed to run from 25 °C to 900 °C at a heating rate of 10 °C/min in the simultaneous thermal analyzer STA 8000 from Perkin Elmer.

2.3 Adsorption essays

2.3.1 Standard preparation

To perform the adsorption essays, six different concentrations of the metal ions were defined at around: 1, 10, 20, 30, 50 and 90 ppm. Table 1 shows the specific concentration used for each metal. Solutions were prepared by dilutions based on total mass rather than volume to obtain a more exact measure of concentration and to avoid possible inconsistencies due to differences in temperature. These concentrations were defined considering that the present research seeks to define the effectivity of the materials in diminishing high heavy metal concentrations.

Table 1. Initial metal-ion solutions prepared for adsorption essays

Standard	Copper [ppm]	Lead [ppm]	Cadmium [ppm]
Std 1	98,2109	78,3633	69,1181
Std 2	49,4933	48,3843	47,2339
Std 3	34,3832	28,0914	30,9795
Std 4	20,2197	19,7704	17,8632
Std 5	8,7203	10,1859	9,1991
Std 6	1,0515	1,0016	1,0079

Table 1 shows the concentrations of the studied metal-ion solutions. Certain differences can be observed among standards, but each one has a known concentration that can be tracked for possible changes after adsorption. These solutions were used as explained below.

2.3.2 Batch adsorption essays

A defined amount of each cellulose was weighted (1, 3 or 5 mg/mL) in order to be tested with 10 mL of each metal-ion solution. These prepared samples were mixed for 1 minute to let adsorption take place. After this, the mixture was centrifuged and separated into its solid and liquid phases. Filtration was also implemented to remove any solids not centrifuged completely. The two phases were stored for their respective

analysis. Additionally, 50mL of the highest concentration solution of each metal were subjected to the commercial water filter; the collected solution was analyzed by AAS.

2.4 Atomic absorption spectroscopy (AAS)

Atomic absorption spectroscopy provides the concentration of elemental metals in solution in comparison to standard solutions. The equipment used is the Buck 210VGP Atomic Absorption Spectrophotometer. The liquid samples go through this analysis in to determine the remaining metal-ion concentration after the adsorption process thus, the quantity of adsorbed metal in the materials. However, considerations before using the equipment include the variability and range of its detection of copper, lead and cadmium. The flame used for the vaporization of the sample is sensitive to wind currents, acetylene and oxidant flow, and sample stream. For these reasons, a calibration curve needs to be generated each time the equipment is used. Even more, each metal has a range of detection, specified in Table 2, that needs to be considered for the analysis of the samples. If the analyzed sample was above the calibration range, a dilution was performed to bring it to range.

Table 2. Flame atomic adsorption concentration ranges

Metal	Lower limit [mg/L]	Upper limit [mg/L]
Copper	0,01	5
Lead	0,16	20
Cadmium	0,02	2

Table 2 shows the limit of detection and the upper limit for linearity of the calibration curves for the quantification of the metals using the equipment mentioned. A slightly higher limit of quantification was defined to ensure detection of the sample.

2.5 Adsorption Isotherm models

The experimental data was fitted to Langmuir and Freundlich isotherm models. These models describe the progression of an adsorption process. Langmuir model, presented in Equation 1, does such by assuming that adsorption happen in a monolayer in a homogeneous

surface, where adsorbed molecules do not interact with one another. If chemisorption, multilayer or cooperative adsorption are present, this model fails. In this sense, Freundlich isotherm, presented in Equation 2, assumes multi-molecular layer adsorption with possible intermolecular interactions in a heterogeneous surface. The graphing and analysis software Origin 2023 from *Originlab* Corp. will be used for model fitting and correlation information. The models were defined in the “user defined” option for fittings in the software, according to Equations 1 and 2.

Equation 1. Langmuir model

$$q = \frac{WK \cdot C}{1 + K \cdot C}$$

Equation 2. Freundlich model

$$q = K_F \cdot C^{1/n_F}$$

After curve fittings, the highest correlation coefficient indicated which set of data fitted each model best. Thus, which set of data had a defined adsorption progression. Since each essay was not performed several times, other statistical analysis will not be done, as some of these methods require population data.

3. RESULTS AND DISCUSSIONS

3.1 Composition analysis of the materials

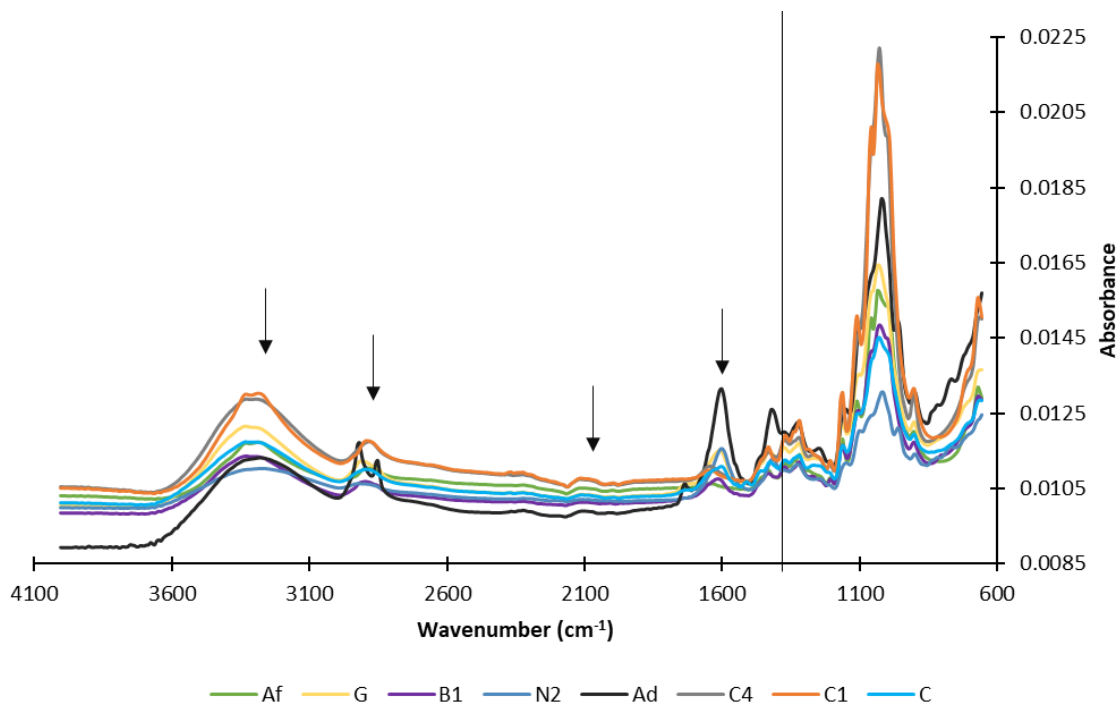


Figure 1. FTIR spectra of extracted materials and commercial cellulose

FTIR spectra provide information on molecular internal structure. Figure 1 shows the spectra for all 8 materials studied with absorbance on the y axis. Most curves have similar tendencies, peaks, and intensities, noting that materials Ad and N2 show the lowest spectra intensities. Within the fingerprint area, the peak at ~ 900 to ~ 1200 cm^{-1} was assigned to a CO, CH, CC and COC stretching ring, characteristic for cellulose, and differs in intensity for some materials. The peak at ~ 3300 cm^{-1} was assigned to OH stretching. The peak at 2900 cm^{-1} was assigned to CH stretching and the last peak at 2100 cm^{-1} was assigned to OH bending, as it is very weak. Finally, peaks around 1600 cm^{-1} are attributed to C=O stretching.

Control materials C1 and C4 displayed the spectra most similar to those of cellulose in literature, setting a reference spectrum for cellulose-rich materials. More intensity in the cellulose fingerprint area can be attributed to higher presence of the assigned atom interactions,

hence, a clear indicator of isolated cellulose in the samples. Among the plotted spectra, sample Ad showed the biggest differences with the other samples, specially at its peak at 1600 cm^{-1} , that is noticeable more intense. This peak even surpasses the peaks around 1400 cm^{-1} , which is an indicator of hemicellulose presence [18]. Furthermore, Ad spectra shows two peaks at $\sim 2900\text{ cm}^{-1}$: at 2917 cm^{-1} and another at 2857 cm^{-1} that could be assigned to CH stretching.

The possible presence of hemicellulose and lignin were considered when assigning the bands and peaks to the functional groups. Even more, a comparison with the results of Morán et al. showed great difference between the results in Figure 1 and lignin spectrum, and major similarities with their cellulose spectrum [18]. Inconsistencies on the spectra were attributed to impurities left from the extraction method or to the chosen analyzed sample not being representative of the whole material. FTIR by itself typically cannot show all the functional groups of biomaterials because of possible overlap of different functional group peaks present in complex material composition. For this reason, these results were complemented with a thermogravimetric analysis (TGA) in an effort to identify the main component or components of the extracted materials. Table 3 displays some of the most relevant findings of this analysis.

Table 3. Temperature of maximum decomposition for main components on the original materials

	Material	Temperature of maximum weight loss rate ($^{\circ}\text{C}$)	Mass loss percentage	Assigned component
Control	C1	340	86.44 %	Cellulose
	Af	346	84.82 %	Cellulose
	C4	355	76.25 %	Cellulose
Extracted	C	317	57.78 %	Cellulose
	Ad	248	20.28 %	Hemicellulose
		287	25.60 %	Cellulose
	B1	235	12.86 %	Hemicellulose
		323	53.51 %	Cellulose
	G	248	12.70 %	Hemicellulose
		338	54.66 %	Cellulose
	N2	248	20.37 %	Hemicellulose
		292	27.01 %	Cellulose

Table 3 contains the temperature of maximum weight loss rate of each sample, the mass loss percentage, and the component assigned to that decomposition. These peaks were obtained with the derivative of the thermal curves of each sample, which can be further examined in Annexes

Annex A: Thermal curves (TGA) and their respective derivatives. The component assignment was based on the work of Bravo et al. and Morán et al. as the analysis environment and method were similar [17], [18]. According to these studies, hemicellulose started its decomposition at 220 °C and continued up to 315 °C, with a decomposition peak at 268 °C. Cellulose, on the other hand, started decomposing at 315 °C and persisted until 400 °C, with a maximum weight loss rate at 355 °C [18]. Regarding the control materials, as they are commercial celluloses, high weight compositions of this polymer were expected.

Materials G, C and B1 had the largest percentage of cellulose (54.66 %, 57.78 % and 53.51 %, respectively) on their composition, even with slight peaks overlap around 290°C, attributed to hemicellulose. On the other hand, material Ad had a distinctive FTIR spectra among the materials and TGA results show that the sample had a significant percentage of hemicellulose. Material C contains a significant amount of cellulose but, similar to material G, it has an overlap with a hemicellulose peak. The presence of hemicellulose was attributed to the execution of the extraction method, especially the treatment meant to eliminate this component from the material. All materials might have some percentage of lignin but, since its decomposition was reported between 200°C and 700°C, the overlap of its decomposition with those of the other materials makes it difficult to identify [18].

Furthermore, TGA analysis showed that all samples had some residual water or small volatile components from the extraction process that decomposed at temperatures below 180°C. Successful drying of the samples is relevant to their application on heavy metal removal because hydration of the material jeopardizes the polarity of cellulose molecules that make

adsorption effective. In this sense, samples Af and Ad had the lowest water content (below 3%) whereas sample N2 had the highest water and small volatile components content (~12%). Based on the previous findings, extracted materials B1 and G are expected to perform the best regarding heavy metal removal and material since their FTIR spectra suggests cellulose-like structure. This was confirmed with TGA, revealing that both materials have a large percentage of cellulose in its composition, and that remaining water and small components were below 6% of their mass.

3.2 Changes in the samples after batch adsorption essays

Heavy metal adsorption on the materials is expected to occur through physical adsorption; metallic cations attach to cellulose surface by weak bonds. After batch adsorption essays, site occupation by the metals is expected to affect electronegative sites in the adsorbent molecules. FTIR spectra was done for the samples after the essays with each metal; these results are presented in Annex B: FTIR spectra before and after adsorption. Control materials (C1, C4 and Af) had minimal or no change in their spectra after adsorption essays. Since no adsorption was expected to happen, the material molecules remained unchanged in the presence of heavy metal ions, and functional groups detected prior to the process remained.

Materials B1 and N2, on the other hand, showed a decrease on peak intensities after adsorption, suggesting the interaction between ions. The most noticeable decrease in peak intensity for this materials spectrum occurred after adsorption essay with copper. N2 spectra in Figure 2 shows that peak intensities for the material after copper adsorption were reduced considerably, in comparison to the results after lead and cadmium essays. Finally, for material Ad, Cu and Cd ions caused similar peak decrease in the spectrum, but material C was, apparently, mostly affected by cadmium presence. Some peak shifts were observed in the presence of metal ions, but more studies are required to determine possible reasons.

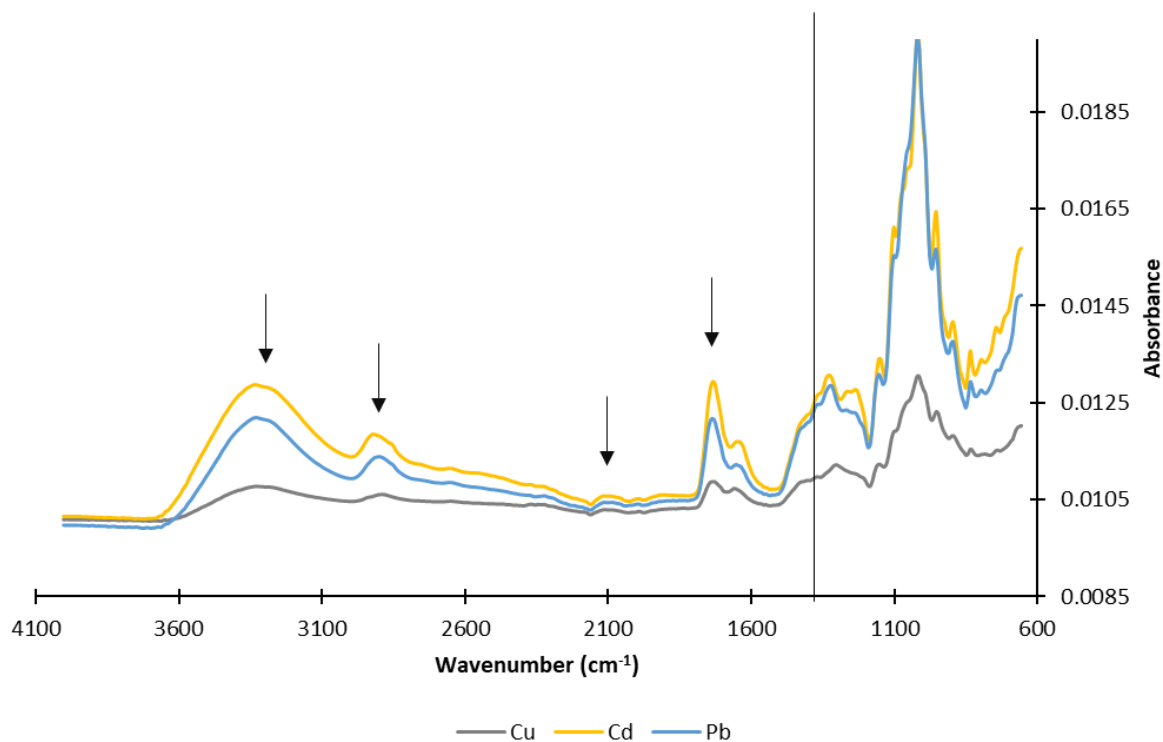


Figure 2. FTIR spectra of material N2 after adsorption essays

3.3 Adsorption Essays

The study of the proposed materials as cellulose sources for heavy metal removal from water is only reported in literature for material N [12]. The remaining 4 sources (B1, C, Ad and G) have not been previously analyzed for this purpose. Figures 3 and 4 show a small sample of the obtained data after the adsorption essays as a plot of percentage of metal remaining in solution when exposing an initial solution of 50 and 10 ppm to 5 mg/mL of cellulose. These sets of data were selected to identify the material that removes the most metal-ions from high initial concentrations. Also, the highest concentration of cellulose was selected for these plots because “the biosorbent amount is a vital factor affecting the removal efficiency due to offering more vacant biosorption sites” [7]. These figures will provide preliminary conclusions on which material is most effective or heavy metal removal by adsorption.

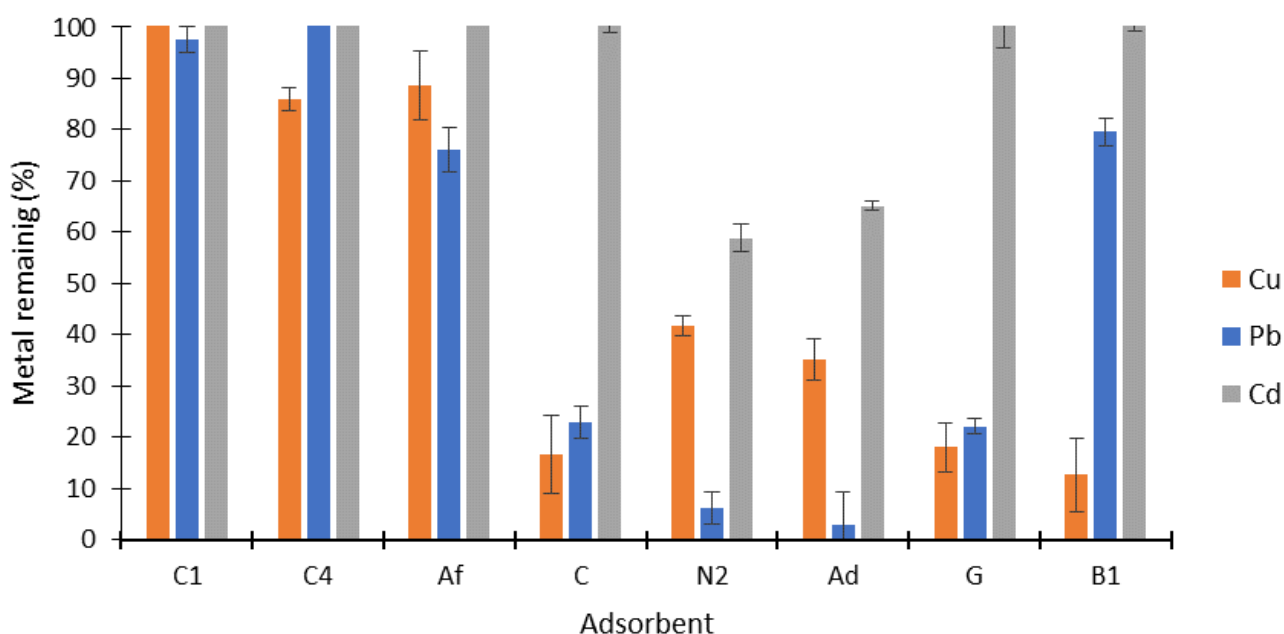


Figure 3. Percentage of metal remaining in solution from initial concentration of 50 ppm using adsorbent at a concentration of 5 mg/mL.

Figure 3 shows a bar graph of the percentage of metal-ion concentration remaining in solution from an initial concentration of 50 ppm, after being exposed to the 8 adsorbent materials present in solution at 5 mg/mL. The y-axis represents the relation between final and initial concentration of the studied solution as a percentage. On the x-axis the codes for the materials are presented, each one assigned with 3 bars corresponding to each of the 3 metals. This graph provides insight into the amount of metal ions removed by the adsorbent, where a higher percentage of remaining metal implies less adsorption in the material. In this sense, cadmium removal was most challenging out of the 3 metals. Control materials, as expected, removed minimal or no metal at all from the original solution, with material Af removing a maximum of 20% of Pb. Material C had no detectable change in cadmium concentration, whereas it removed around 80% of copper and lead. N2 showed the least removal amount of cadmium and copper (around 45%) but eliminated almost 90% of lead.

Material Ad removed a high percentage of lead from the sample ($\sim 90\%$) but low percentages of copper and cadmium (60 and 40% respectively). Both materials G and B1 had no detectable removal of cadmium but removed around 20% of copper. Regarding lead, material B1 only removed 20% of initial metal, while material G removed 75%. It must be noted that all these results are only true for the specified data used to generate Figure 3 ($C_0=50$ ppm and $C_C=5$ mg/mL).

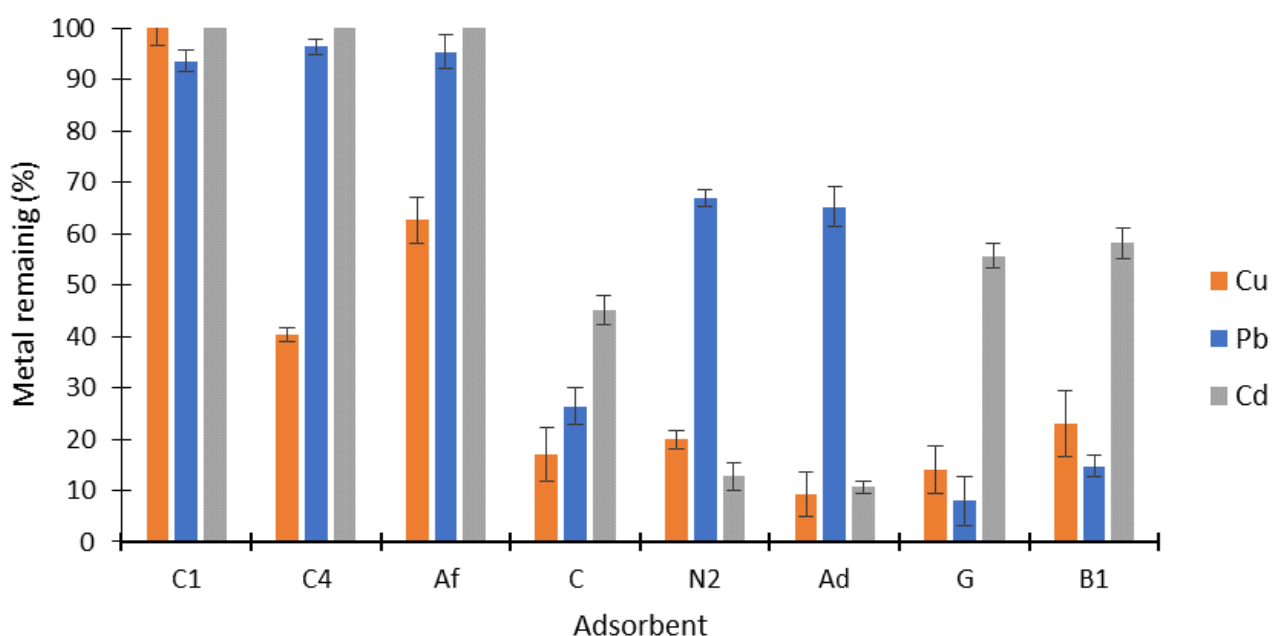


Figure 4. Percentage of metal remaining in solution from initial concentration of 10 ppm using adsorbent at a concentration of 5 mg/mL.

Figure 4 shows a bar graph of the percentage of metal remaining in a solution of original concentration of 10 ppm, after being exposed to the 8 adsorbent materials present in solution at 5 mg/mL. Control materials, as expected, removed some or no metal at all from the original solution, with materials Af and C4 removing around 50% of initial copper. Regarding the extracted materials, remaining metal is noticeable lower with $C_0=10$ ppm than with $C_0=50$ ppm, especially for cadmium metal. Materials C, G and B1 had around 50% of cadmium remaining in solution, but only around 20% of copper. Lead removal with C was around 70%

and with G and B1, around 85%. Materials N2 and Ad had a high percentage of lead remaining in solution (~ 70%) but low percentage of cadmium remaining (~ 15%), and both materials removed around 25% of copper. It must be noted that these results are only true for the specified data used to generate Figure 4 ($C_0= 10$ ppm and $C_C= 5$ mg/mL).

Overall, cadmium removal was low with every material at both concentrations but N2 and Ad were one of the most effective in both cases. On the contrary, apart from control materials, B1 removed the least amount of cadmium from solution. Regarding copper, materials C and G removed around 80% of the metal for both initial concentrations. However, all extracted materials showed similar effectiveness for this metal. For lead, Figures 3 and 4 suggest that there is more removal of metal with higher initial concentrations, since materials N2 and Ad had around 70% of metal remaining with $C_0= 10$ ppm, but only 10% with $C_0= 0$ ppm. The theoretical models proposed disagree with this behavior, as they suggest that higher initial concentrations produce higher percentage of metal remaining in solution or, similarly, produce lower removal percentages. Sections 3.3.1 to 3.3.3 investigate on model fitting to the obtained data. However, adsorption isotherm models, in some cases, did not adjust for the obtained data, meaning that Originlab software was unable to fit the models to the process. This could be attributed to high variability of the results, that require several repetitions of the essays to obtain statistically significant results or to other factors regarding the adsorption process itself.

On the other hand, materials N2 and Ad were effective for both sets of data on heavy metal removal. These materials, however, were identified to have high percentages of hemicellulos on their composition, suggesting that cellulose alone might not be effective for these metals' removal from water. This is further reinforced with the minimal removal percentages of control materials C1, C4 and Af, whose main component is cellulose. However,

work should be done to control the existence of hemicellulose and confirm its effect on heavy metal adsorption. Also, examination on the materials composition and crystallinity can be done in order to ensure the presence and characteristics of cellulose in the materials. Even more, a comparative analysis using hemicellulose as the main component of the materials could expand on whether this component is more effective than cellulose, or if their joint presence is better for heavy metal removal.

Other reasons causing the presented results include surface area and porosity of the material. In the present research material surface area and porosity could not be measured due to the lack of access to the equipment but further studies are necessary to quantify these values. Additionally, only initial metal concentration and identity, and adsorbent dose were assessed in this investigation. Supplementary information could be obtained by changing contact time, pH and temperature.

Extracted materials had different effectiveness in removing different metals when exposed at the same conditions. Material B1, for example, removed almost 80% of copper but only 20% of lead but material (at $C_0=50\text{ppm}$). This suggests that cellulose from different sources used simultaneously could remove considerable amounts of the metals from water. More studies should be done by combining the extracted materials and the selected heavy metals to obtain further information.

Two additional control settings were studied to determine effectivity of the extracted materials. These consisted of exposing an initial metal solution of 70 ppm to a commercial water filter (FI) and 5mg/mL of activated charcoal (CA). The commercial filter is composed of activated charcoal from coconut husk, zeolite and an ionic-exchange membrane, all 3 very common methods of metal remediation. The results for these essays are presented on table.

Table 4. Percentage of metal remaining in solution from initial concentration of 70 ppm using activated carbon and a commercial water filter

Metal	Material	Remaining metal in solution
Cu	FI	45.57 %
	CA	81.34 %
Pb	FI	50.76 %
	CA	93.69 %
Cd	FI	63.97 %
	CA	100.00 %

Table 4 shows metal remaining in solution after exposing the initial solution to FI and CA. Activated charcoal was not effective for metal adsorption, providing results similar to those obtained with the control materials in the set of data for Figure 3. The commercial filter, however, removed between 40 and 50% of metal present in solution. Regarding previous results from figure 2, cadmium removal with FI is higher than with the extracted materials. This is attributed to the presence of 3 different metal-removal methods inside the filter.

Nevertheless, materials C, G and B1 proved to be more efficient in Pb and Cu removal from water than FI. The commercial filter, even with 3 different methods of purification, had higher concentrations of Pb and Cu metals remaining in solution. For cadmium, nonetheless, the filter removed more metal than the extracted materials for initial concentration of 70 ppm. At lower concentrations, materials N2 and Ad had small percentages of metal remaining in solution, so further experimentation could be done to optimize the use of these materials in Cd removal from water.

3.4 Isotherm studies

3.4.1 Copper

Table 5. Summary of model fitting results

Material	Cellulose concentration	Model	R²
C4	3 mg/mL	Langmuir	0.99187
G	1 mg/mL	Freundlich	0.97208
C1	3 mg/mL	Freundlich	0.34444
B1	1 mg/mL	Freundlich	0.54764

Table 5 shows the best and worst model fitting for copper essays, that were selected after fitting both models to the data and selecting the best fit for each data set. Complete results can be examined in Annex D: Summary of Curve fittings to isotherm models. Extracted material G had the best model adjustment to its data, and material B1 the worst. Both materials were high in cellulose content, so the model fitting can not be explained by material composition. Furthermore, model fittings for control materials C4 and C1 were also undefined by cellulose presence. Poor model fitting is explained by high variability of the data caused by the AAS method. Several repetitions of the essays should be performed to obtain statistically significant results. Furthermore, since the sensibility of the equipment has a very limited detection range for this metal (between 0.01 and 5 ppm) almost every sample had to be diluted before analyzed. This procedure most likely introduced errors in the results, causing the presented results. Other factors that might have affected curve fittings include possible chemisorption, deposition of the metal-ions in the porous surfaces, adsorbate interactions, or to other factors regarding the adsorption process itself.

3.4.2 Lead

Table 6. Summary of model fitting results

Material	Cellulose concentration	Model	R²
G	3 mg/mL	Langmuir	0.97844
G	1 mg/mL	Freundlich	0.67025

Table 6 shows the best and worst model fitting for lead essays, that were selected after fitting both models to the data and selecting the best fit for each data set. Complete results can be examined in Annex 3. Extracted material G had the best and worst model adjustment to its data. This material was high in cellulose content, so the model fitting can not be explained by material composition. Poor model fitting is then explained by high variability of the data caused by the detection AAS method. Several repetitions of the essays should be performed to obtain statistically significant results. Furthermore, large range of detection might have impacted the precision of data collection, making the information to be scattered and limiting model fitting. Other factors that might have affected include possible chemisorption, deposition of the metals in the porous surfaces or to other factors regarding the adsorption process itself.

3.4.3 Cadmium

Table 7. Summary of model fitting results

Material	Cellulose concentration	Model	R²
C4	3 mg/mL	Langmuir	0.9902
B1	1 mg/mL	Langmuir	0.9731
C1	5 mg/mL	Langmuir	0.24156
N2	3 mg/mL	Freundlich	0.68494

Table 7 shows the best and worst model fitting for lead essays, that were selected after fitting both models to the data and selecting the best fit for each data set. Complete results can be examined in Annex 3. Extracted material B1 had the best model adjustment to its data, contrary to results for copper data. Material N2 had the worst model fitting adjustment. This material had mixed composition with cellulose and hemicellulose, but control material C1 with high cellulose content had unsuccessful model fitting, so good model fitting can not be explained by material composition. Poor model fitting is then explained by high variability of the data caused by the detection AAS method. Several repetitions of the essays should be

performed to obtain statistically significant results. Furthermore, since the sensibility of the equipment has a very limited range for this metal (between 0.02 and 2 ppm) almost every sample had to be diluted before analyzed. This procedure introduced errors in the results, preventing successful model fitting. Other factors that might have affected include possible chemisorption, deposition of the metals in the porous surfaces or to other factors regarding the adsorption process itself.

4. CONCLUSIONS AND RECOMMENDATIONS

Bioadsorption using cellulose from natural sources is an unexplored method of heavy metal removal in Ecuador. The present document studied 5 materials found in the country as cellulose sources. The extraction process proved to be crucial for the obtention of meaningful and accurate information on the sources, and uncaredful execution of this step affected batch adsorption essays and results. Composition analysis of the materials revealed that some of the extracted samples had complex compositions, having significant presence of hemicellulose. Following this, theoretical model fittings were not dependent on material composition, but rather on the metal detection process. Curve fittings to the proposed models failed for some sets of data, which was attributed to the variability of the results. Performing batch essays in triplicate could provide statistically significant results that better follow theoretical isotherms.

Commercially available cellulose, according to the presented results, does not remove heavy metals from water. Alternatively, metal remaining in solution appeared to decrease in the presence of materials with complex compositions, being materials Ad and N2 the most efficient in removing Cu, Cd and Pb at different initial concentration when $C_c = 5$ mg/mL. The presented results also suggest that metal-ion removal could be specific for the pairing metal-extracted material. Comparative analysis of adsorption using activated carbon and a commercial water filter showed that the available carbon did not remove heavy metals. On the

other hand, the water filter removed about 50% of the studied metals, but some extracted materials had similar removal percentages.

The results of this research provided insight into materials with possible applications in adsorption processes. A comparison was done with a commercial water filter, showing that the extracted materials removed more copper and lead from solution than the product. All the presented analysis were done regarding controlled and artificial heavy metal solutions, very different from real water sources. Further research should focus on real water samples collected from sources affected by heavy metal presence. Also, as ongoing research, more essays will be done towards the regeneration and reuse of the materials, hoping to prove the process is environmentally safe all around.

5. REFERENCES

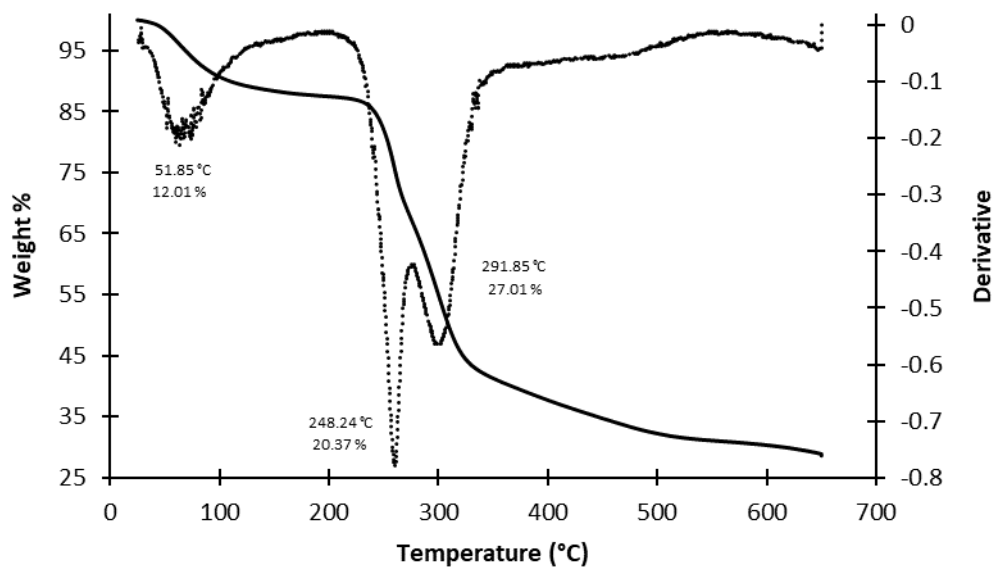
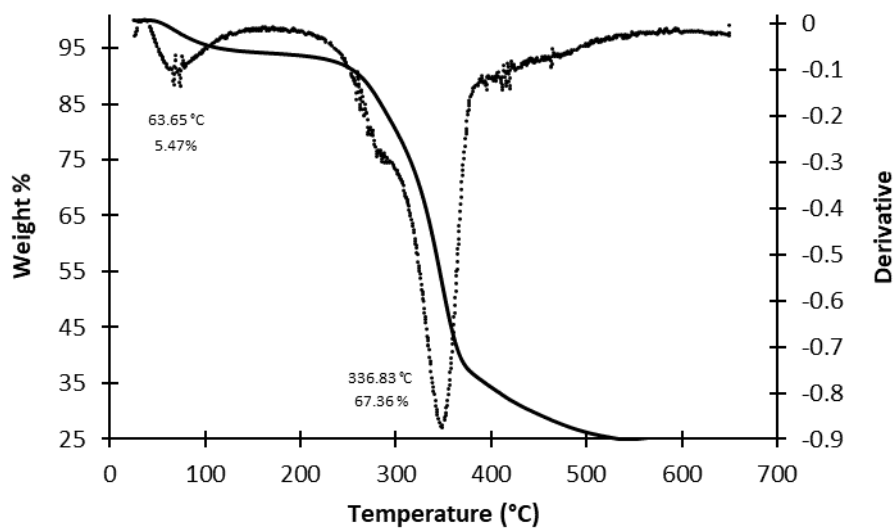
- [1] S. Mitra *et al.*, “Impact of heavy metals on the environment and human health: Novel therapeutic insights to counter the toxicity,” *J King Saud Univ Sci*, vol. 34, no. 3, p. 101865, Apr. 2022, doi: 10.1016/J.JKSUS.2022.101865.
- [2] Health Canada, “Copper in drinking water: Guideline technical document for consultation,” *Government of Canada*, May 25, 2018. <https://www.canada.ca/en/health-canada/programs/consultation-copper-drinking-water/document.html#2.0> (accessed Oct. 02, 2022).
- [3] World Health Organization, “Lead poisoning,” Aug. 31, 2022. <https://www.who.int/news-room/fact-sheets/detail/lead-poisoning-and-health> (accessed Sep. 24, 2022).
- [4] M. T. Hayat, M. Nauman, N. Nazir, S. Ali, and N. Bangash, “Environmental Hazards of Cadmium: Past, Present, and Future,” *Cadmium Toxicity and Tolerance in Plants: From Physiology to Remediation*, pp. 163–183, Jan. 2019, doi: 10.1016/B978-0-12-814864-8.00007-3.
- [5] J. Olivero-Verbel, N. Alvarez-Ortega, M. Alcala-Orozco, and K. Caballero-Gallardo, “Population exposure to lead and mercury in Latin America,” *Curr Opin Toxicol*, vol. 27, pp. 27–37, Sep. 2021, doi: 10.1016/J.COTOX.2021.06.002.
- [6] M. V. Capparelli *et al.*, “An integrative approach to identify the impacts of multiple metal contamination sources on the Eastern Andean foothills of the Ecuadorian Amazonia,” *Science of The Total Environment*, vol. 709, p. 136088, Mar. 2020, doi: 10.1016/J.SCITOTENV.2019.136088.

- [7] N. A. A. Qasem, R. H. Mohammed, and D. U. Lawal, "Removal of heavy metal ions from wastewater: a comprehensive and critical review," *NPJ Clean Water*, vol. 4, no. 1, pp. 1–15, Jul. 2021, doi: 10.1038/s41545-021-00127-0.
- [8] G. M. Gadd, "Biosorption: Critical review of scientific rationale, environmental importance and significance for pollution treatment," *Journal of Chemical Technology and Biotechnology*, vol. 84, no. 1, pp. 13–28, 2009, doi: 10.1002/JCTB.1999.
- [9] C. F. Carolin, P. S. Kumar, A. Saravanan, G. J. Joshiba, and M. Naushad, "Efficient techniques for the removal of toxic heavy metals from aquatic environment: A review," *J Environ Chem Eng*, vol. 5, no. 3, pp. 2782–2799, Jun. 2017, doi: 10.1016/J.JECE.2017.05.029.
- [10] A. Jamshaid *et al.*, "Cellulose-based Materials for the Removal of Heavy Metals from Wastewater – An Overview," *ChemBioEng Reviews*, vol. 4, no. 4, pp. 240–256, 2017, doi: 10.1002/CBEN.201700002.
- [11] Q. Wang *et al.*, "Efficient removal of Pb(II) and Cd(II) from aqueous solutions by mango seed biosorbent," *Chemical Engineering Journal Advances*, vol. 11, Aug. 2022, doi: 10.1016/J.CEJA.2022.100295.
- [12] I. Licona-Aguilar *et al.*, "Reutilization of waste biomass from sugarcane bagasse and orange peel to obtain carbon foams: Applications in the metal ions removal," *Science of The Total Environment*, vol. 831, p. 154883, Jul. 2022, doi: 10.1016/J.SCITOTENV.2022.154883.
- [13] J. E. James and H. I. Maarof, "Production of cellulose from sugarcane bagasse for adsorption of copper ions," *Desalination Water Treat*, vol. 257, pp. 204–212, 2022, doi: 10.5004/DWT.2022.28173.

- [14] J. F. Campaña-Pérez, P. Portero Barahona, P. Martín-Ramos, and E. J. Carvajal Barriga, “Ecuadorian yeast species as microbial particles for Cr(VI) biosorption,” *Environmental Science and Pollution Research*, vol. 26, no. 27, pp. 28162–28172, Sep. 2019, doi: 10.1007/S11356-019-06035-8/FIGURES/4.
- [15] N. Vela-García, M. C. Guamán-Burneo, and N. P. González-Romero, “Efficient bioremediation from metallurgical effluents through the use of microalgae isolated from the amazonic and highlands of Ecuador,” *Revista Internacional de Contaminacion Ambiental*, vol. 35, no. 4, pp. 917–929, 2019, doi: 10.20937/RICA.2019.35.04.11.
- [16] J. I. Caicho Caranqui, L. Ramirez, and F. Alexis, “Development of a cellulose based membrane extracted from the biodiversity of Ecuador to purify water by heavy metals.,” Trabajo de integración curricular presentado como requisito para la obtención del título de Ingeniería Biomédico, Universidad de investigación de tecnología experimental YACHAY, Urcuquí, 2022.
- [17] I. Bravo *et al.*, “Cellulose particles capture aldehyde VOC pollutants,” *RSC Adv*, vol. 10, no. 13, pp. 7967–7975, Feb. 2020, doi: 10.1039/D0RA00414F.
- [18] J. I. Morán, V. A. Alvarez, V. P. Cyras, and A. Vázquez, “Extraction of cellulose and preparation of nanocellulose from sisal fibers,” *Cellulose*, vol. 15, no. 1, pp. 149–159, Feb. 2008, doi: 10.1007/S10570-007-9145-9/FIGURES/10.
- [19] D. Harris, *Quantitative Chemical Analysis*, Eight. New York: Clancy Marshall, 2010.

6. ANNEXES

Annex A: Thermal curves (TGA) and their respective derivatives

*Figure 5. TGA curves for material N2**Figure 6. TGA curves for material G*

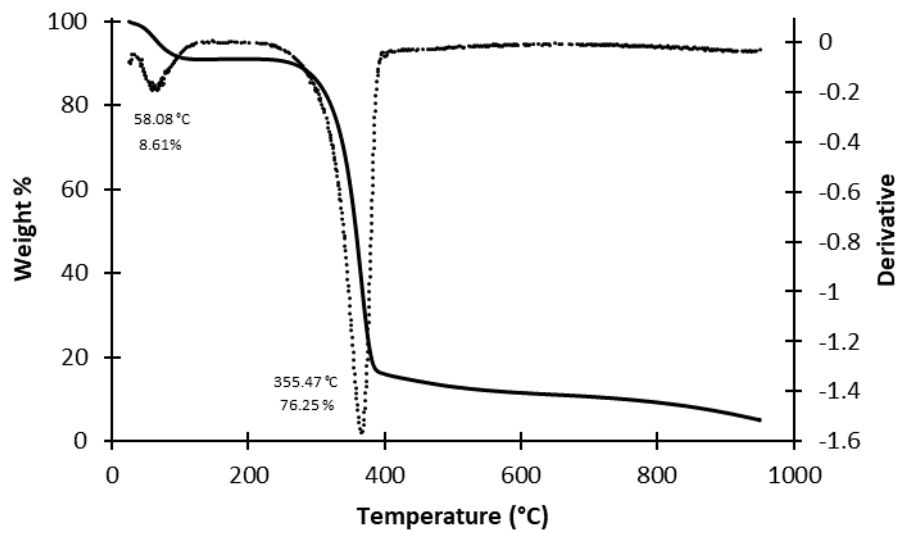


Figure 7. TGA curves for material C4

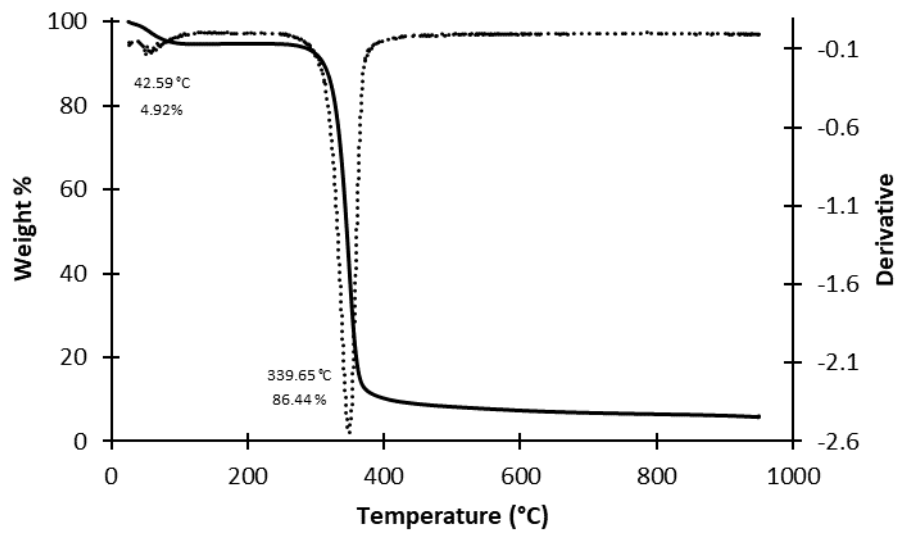


Figure 8. TGA curves for material C1

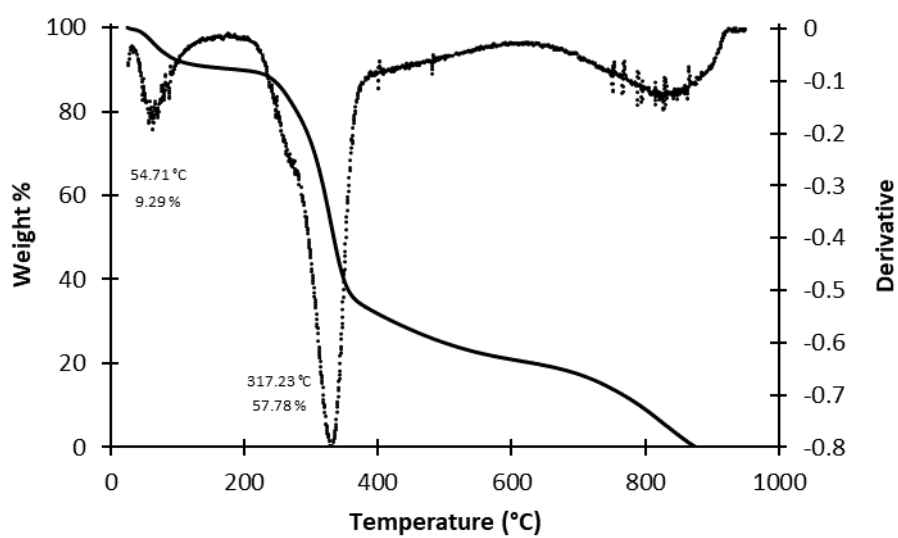


Figure 9. TGA curves for material C

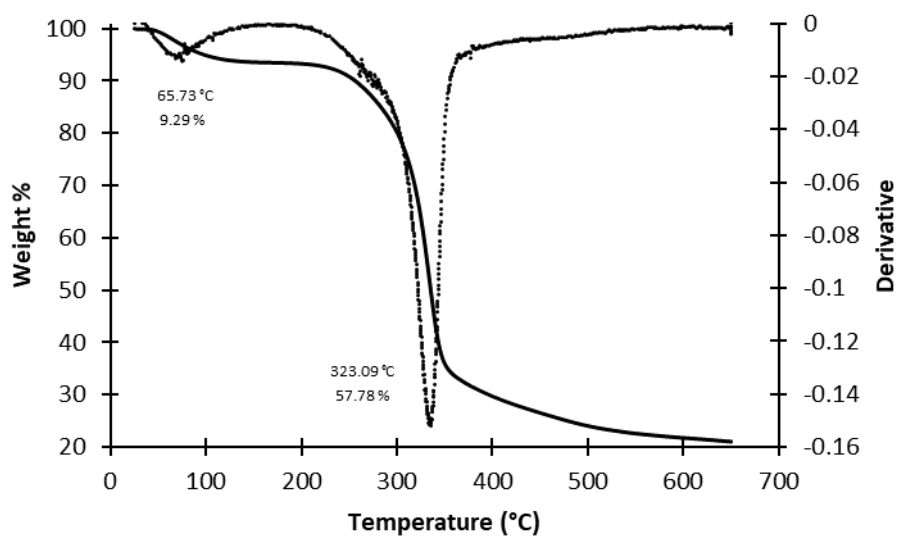


Figure 10. TGA curves for material B1

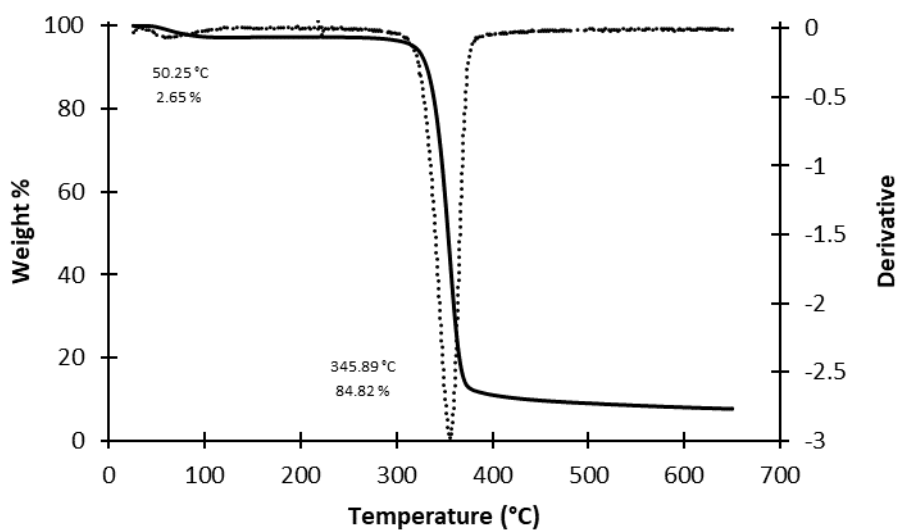


Figure 11. TGA curves for material Af

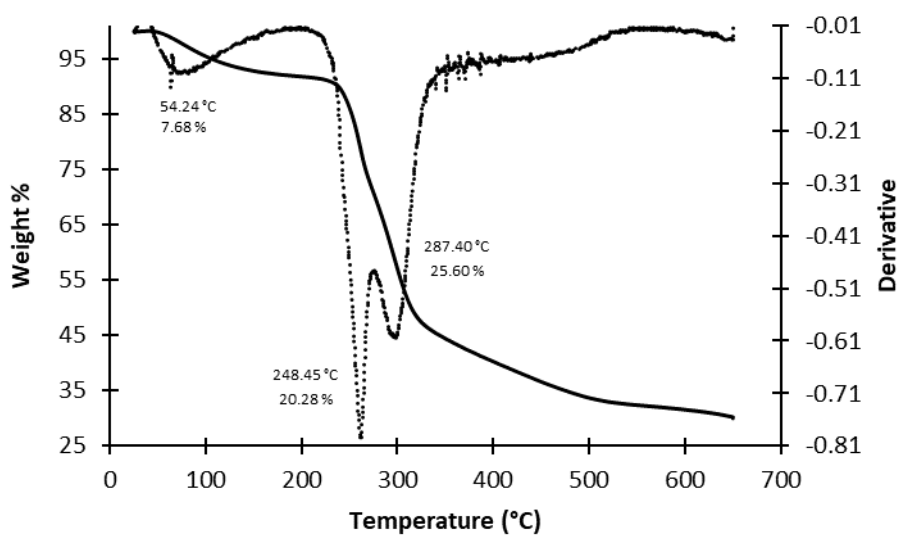
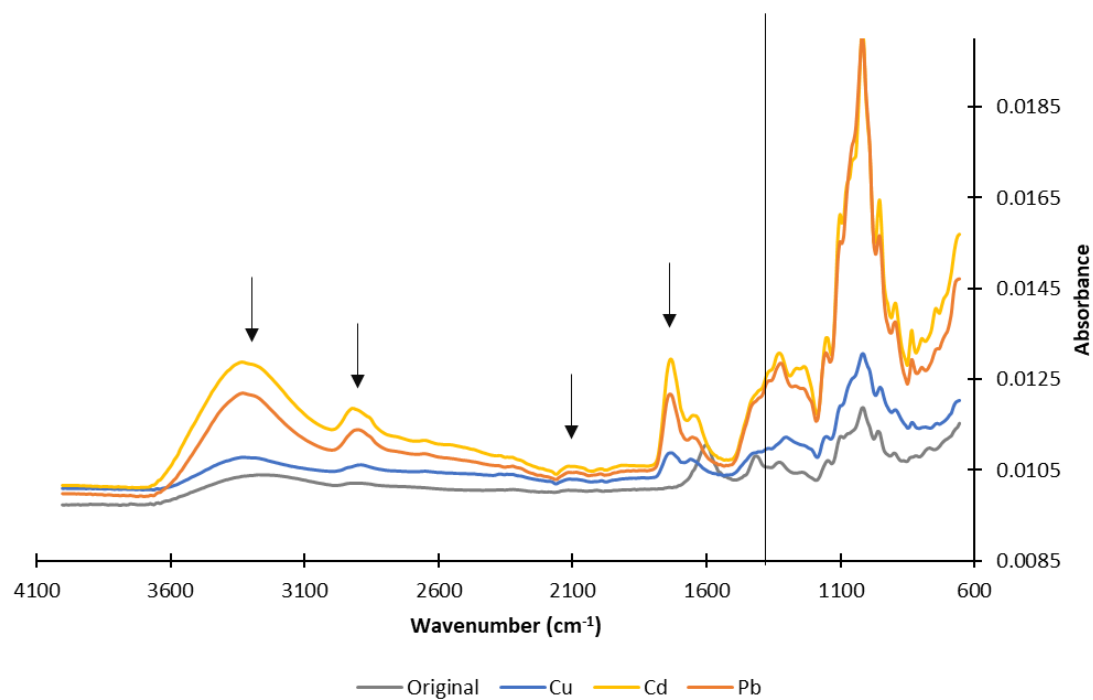
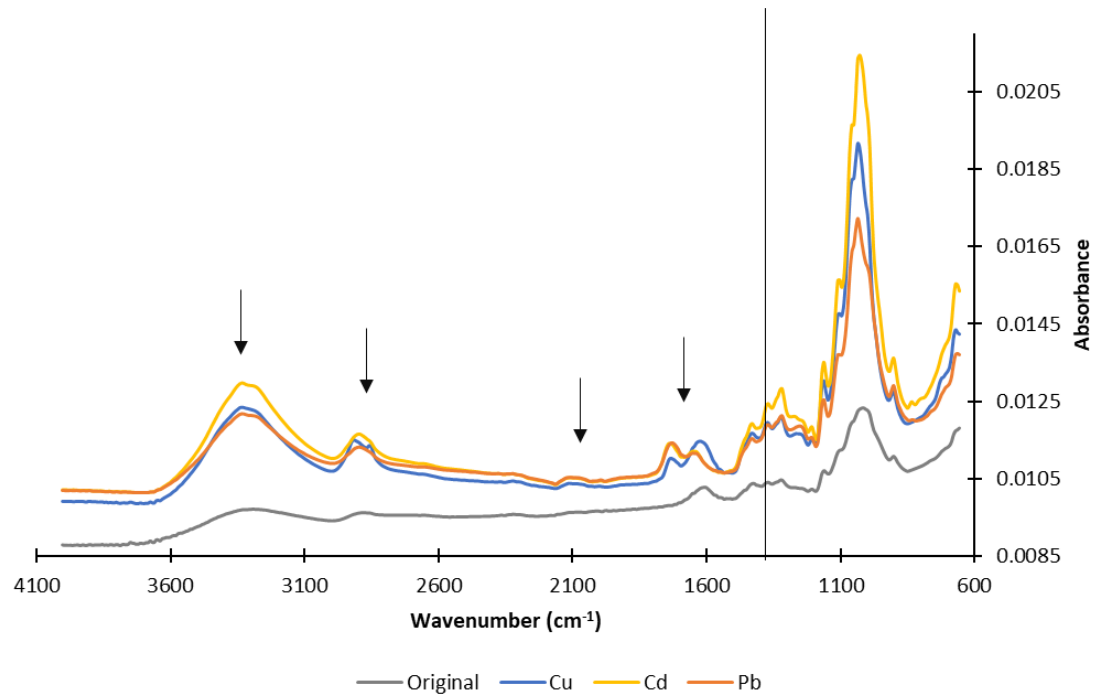


Figure 12. TGA curves for material Ad

Annex B: FTIR spectra before and after adsorption*Figure 13. FTIR spectra for material N2**Figure 14. FTIR spectra for material G*

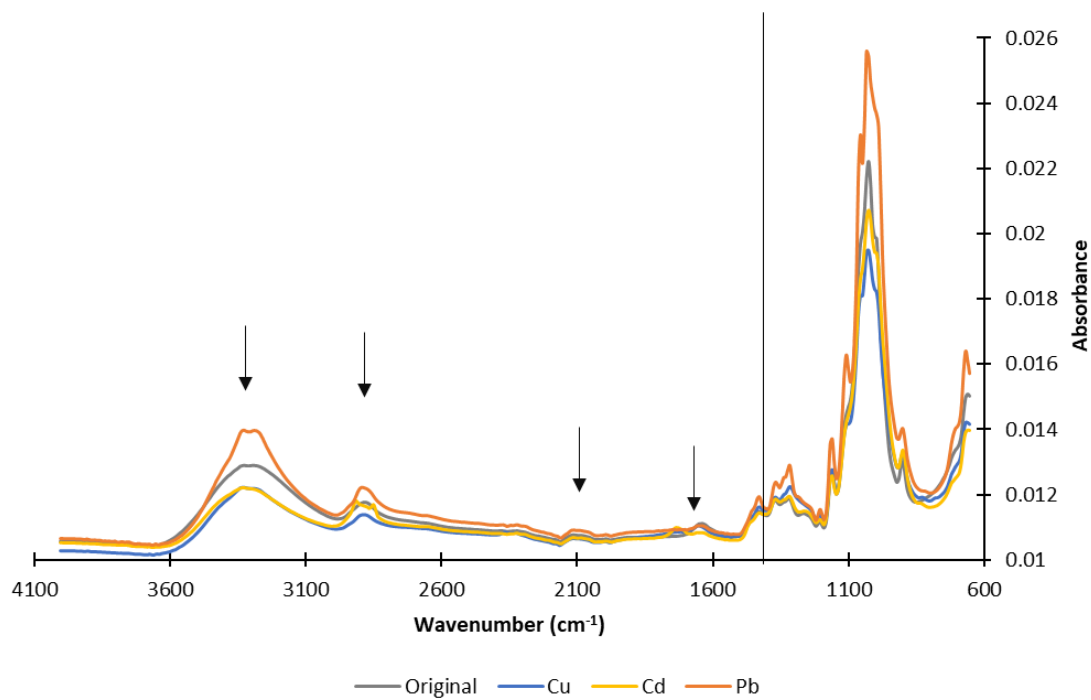


Figure 15. FTIR spectra for material C4

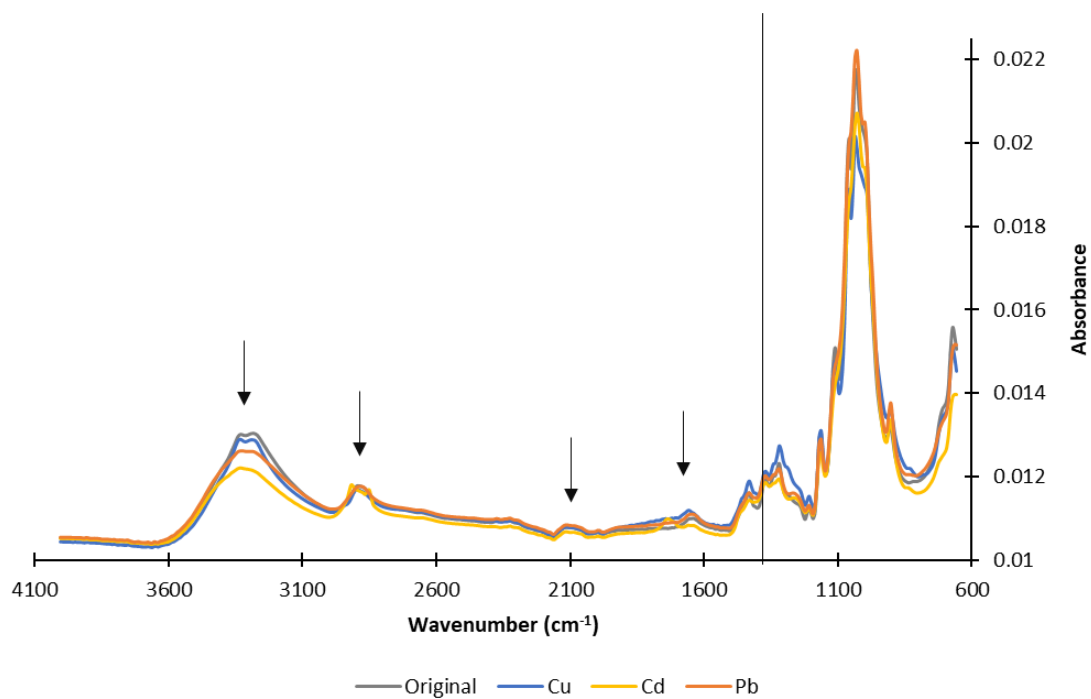


Figure 16. FTIR spectra for material C1

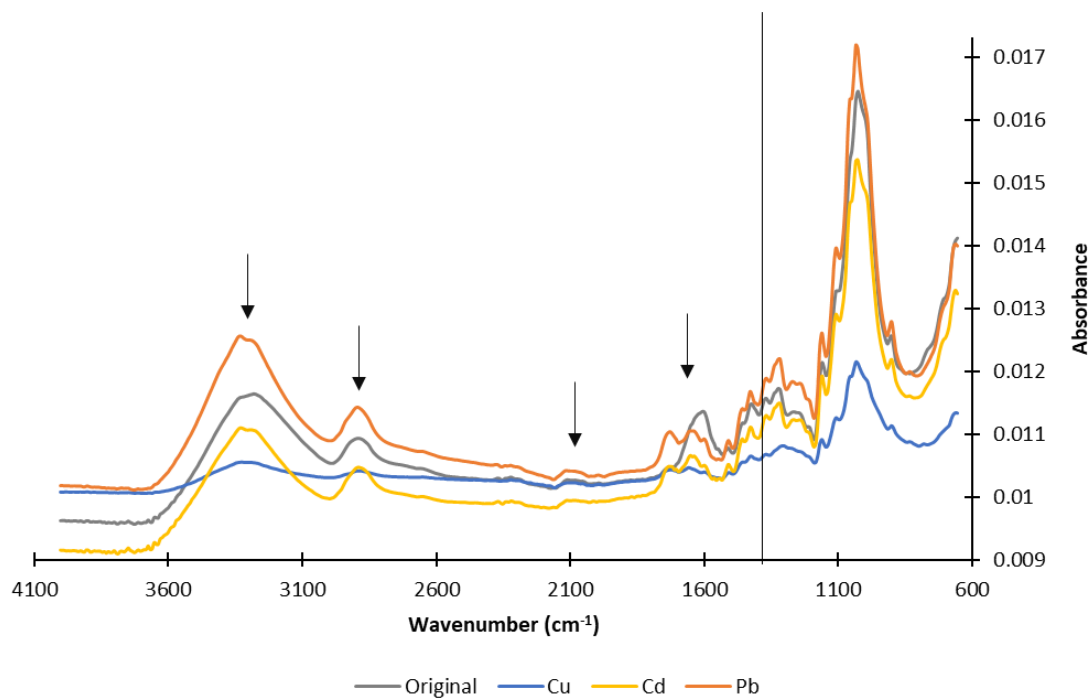


Figure 17. FTIR spectra for material C

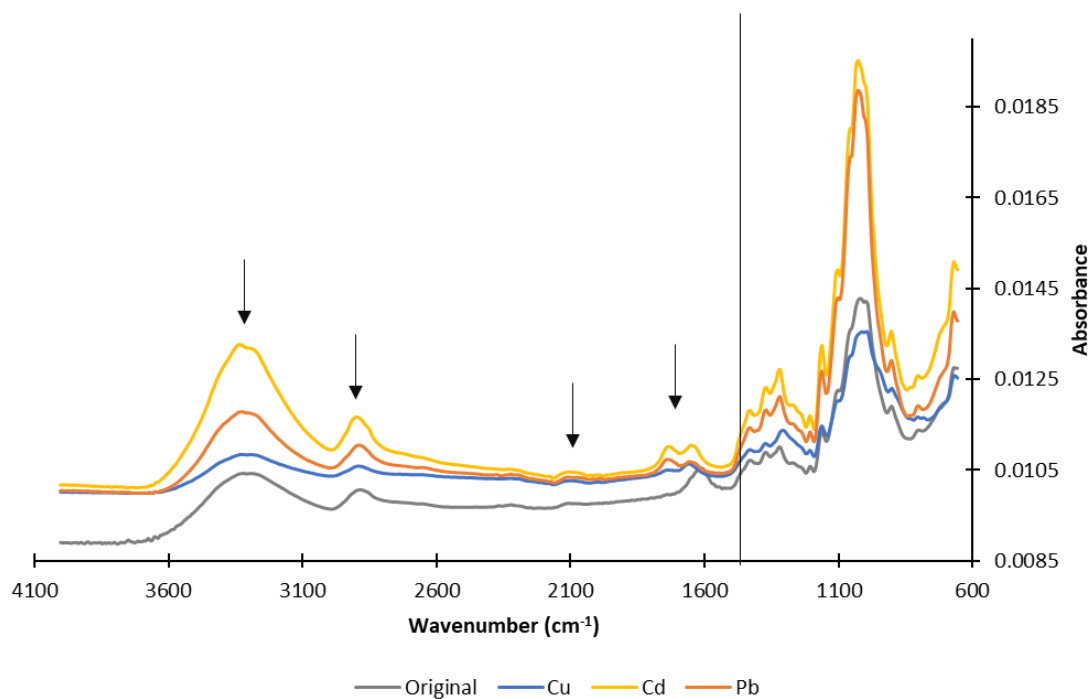


Figure 18. FTIR spectra for material B1

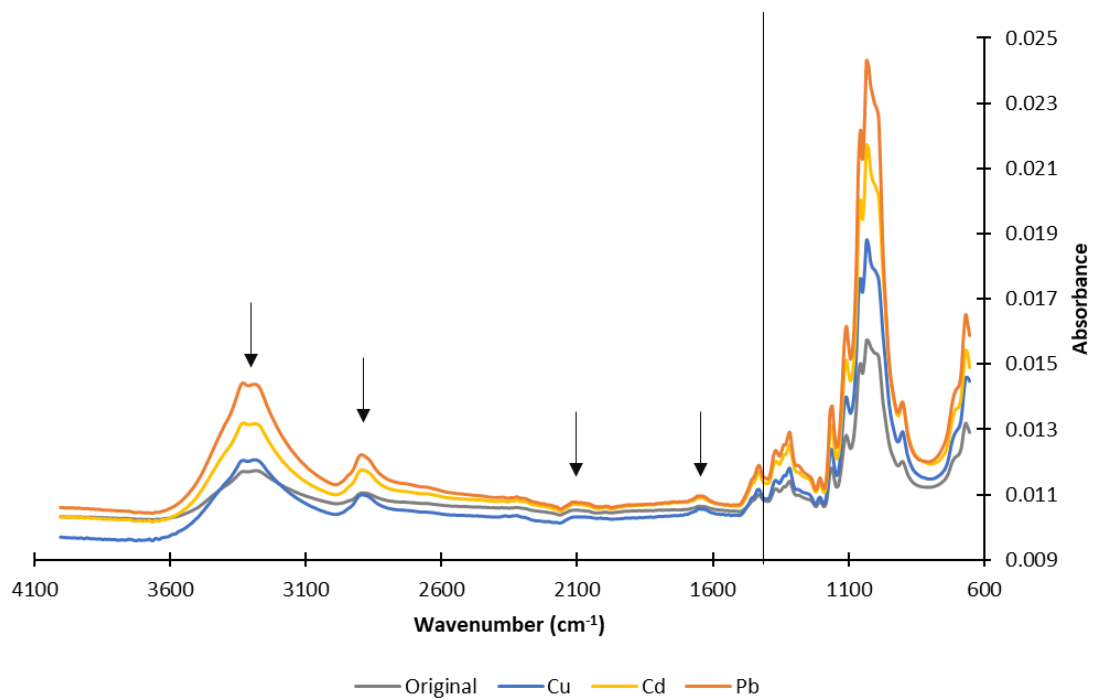


Figure 19. FTIR spectra for material Af

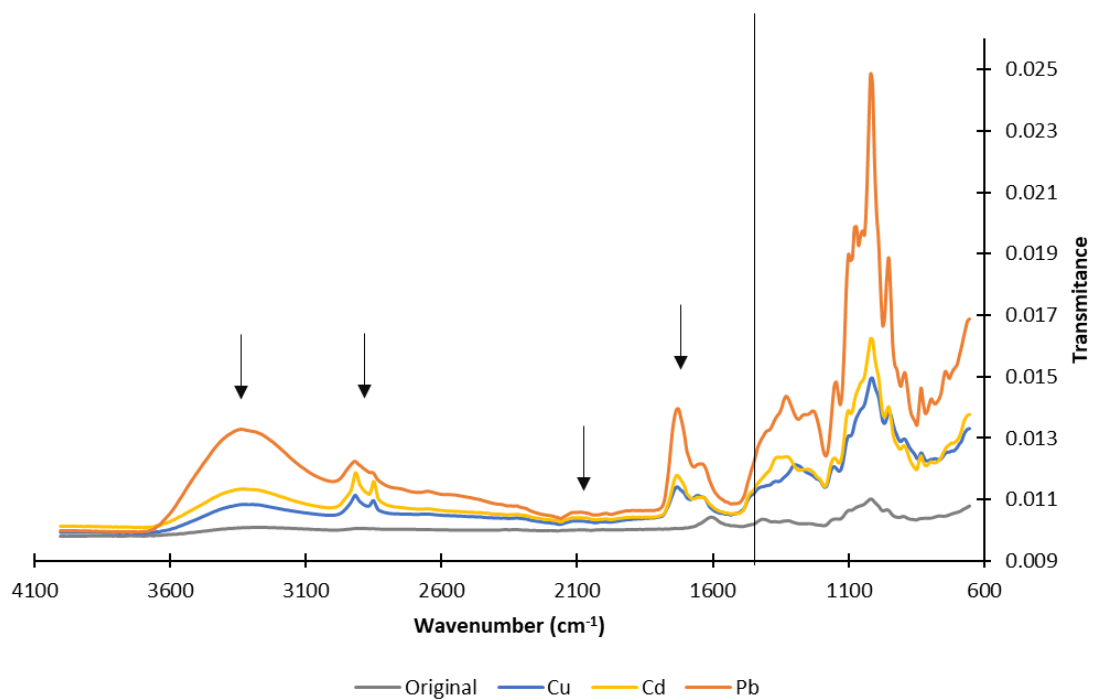


Figure 20. FTIR spectra for material Ad

Annex C: Curve fitting graphs to isotherm models

Copper essays

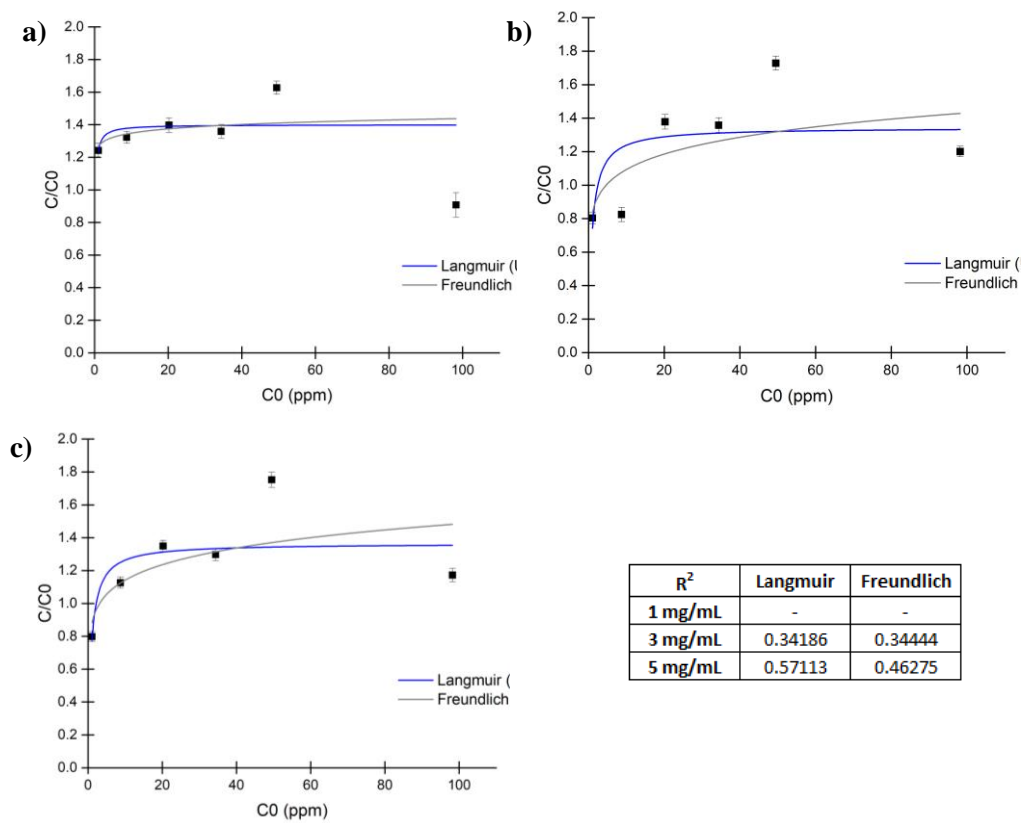


Figure 21. Curve fittings for material C1 with cellulose concentration of a) 1mg/mL b) 3 mg/mL and c) 5 mg/mL

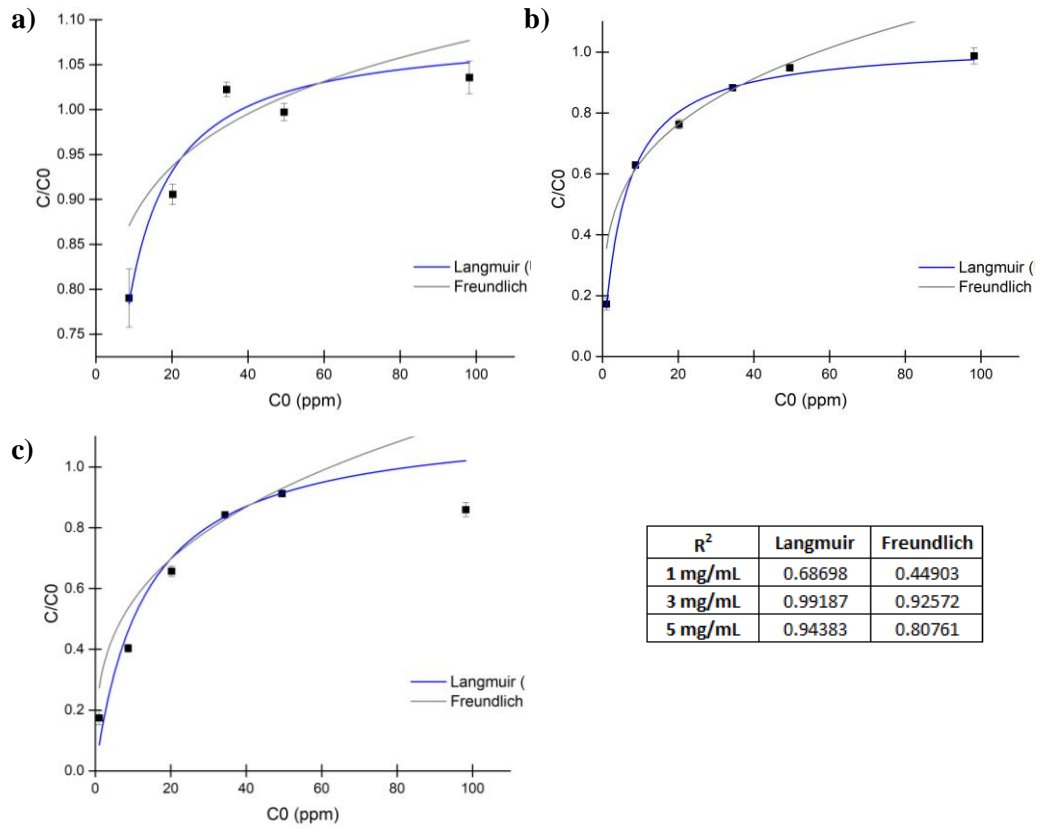


Figure 22. Curve fittings for material C4 with cellulose concentration of a) 1mg/mL b) 3 mg/mL and c) 5 mg/mL

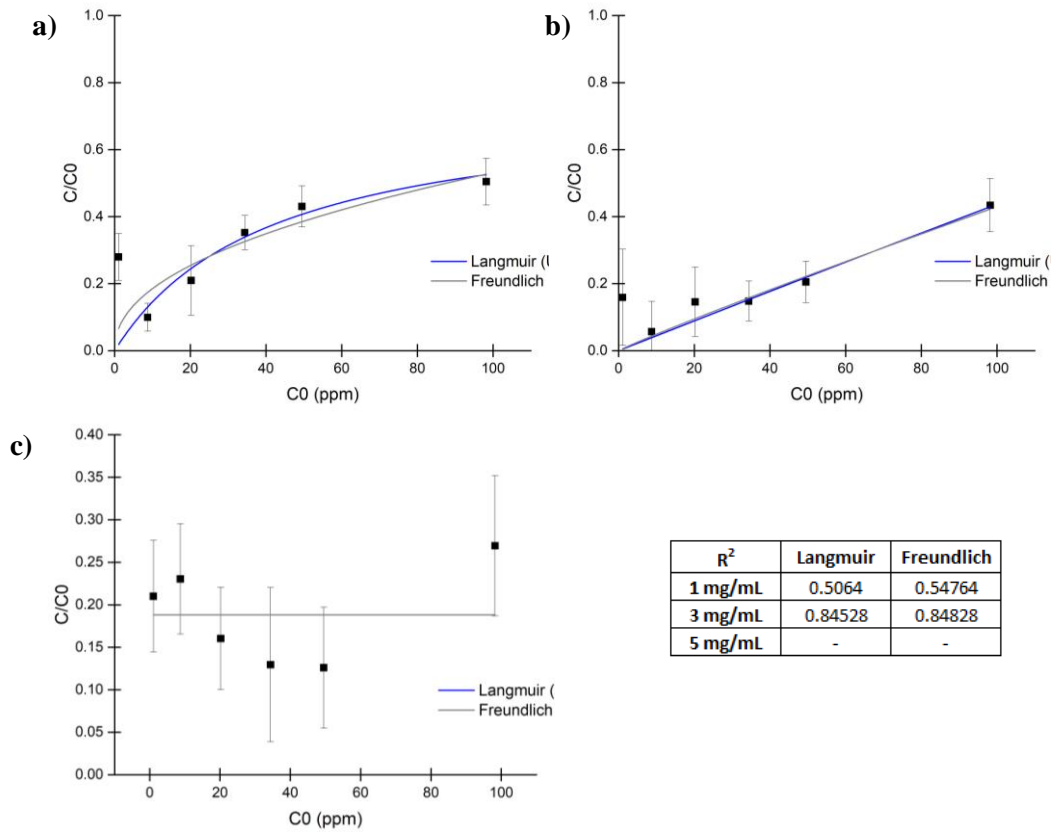


Figure 23. Curve fittings for material B1 with cellulose concentration of a) 1mg/mL b) 3 mg/mL and c) 5 mg/mL

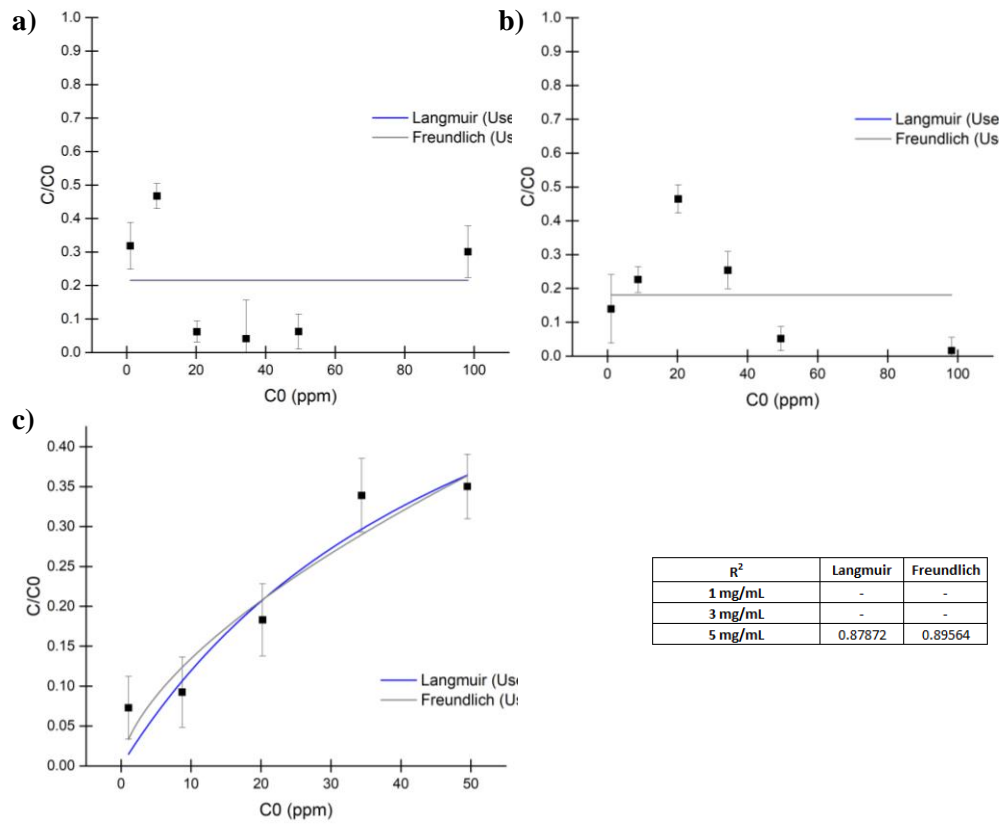


Figure 24. Curve fittings for material Ad with cellulose concentration of a) 1mg/mL b) 3 mg/mL and c) 5 mg/mL

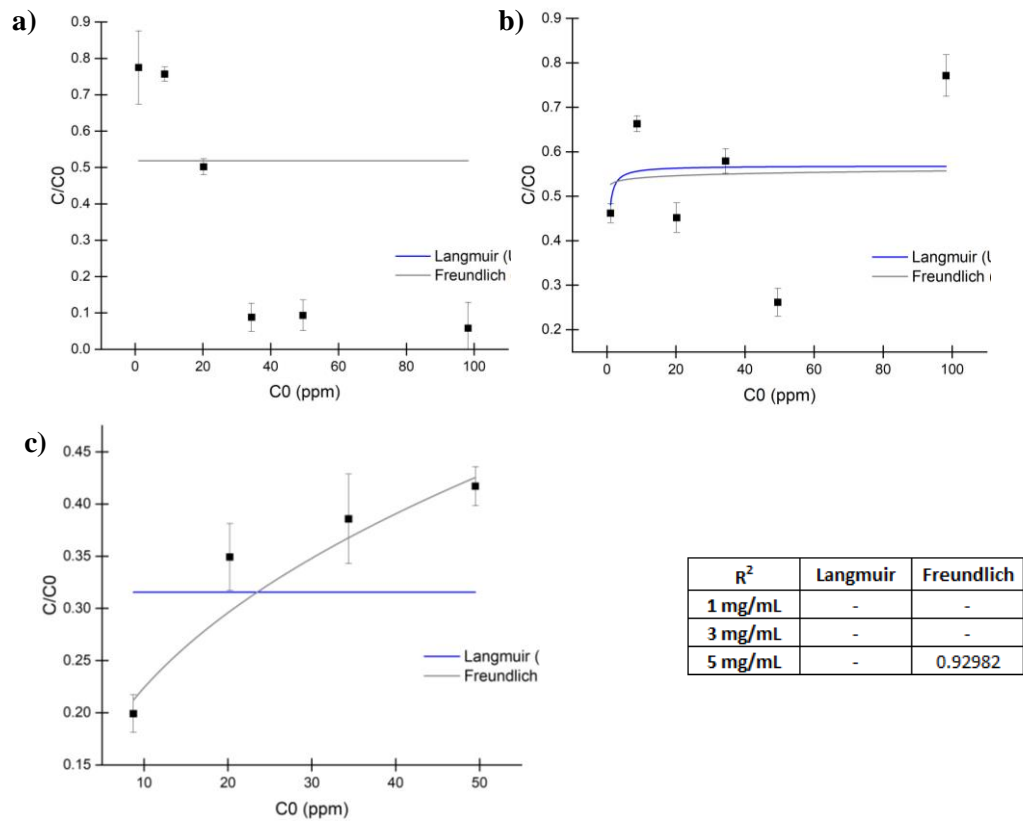


Figure 25. Curve fittings for material N2 with cellulose concentration of a) 1mg/mL b) 3 mg/mL and c) 5 mg/mL

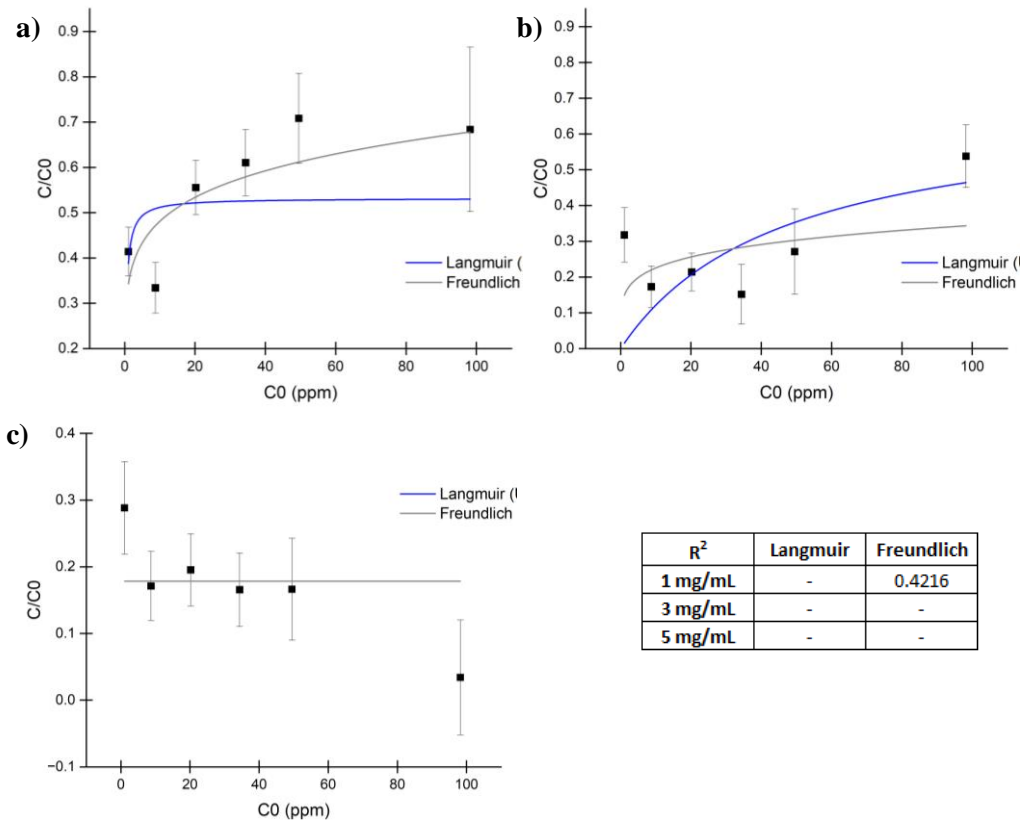


Figure 26. Curve fittings for material C with cellulose concentration of a) 1mg/mL b) 3 mg/mL and c) 5 mg/mL

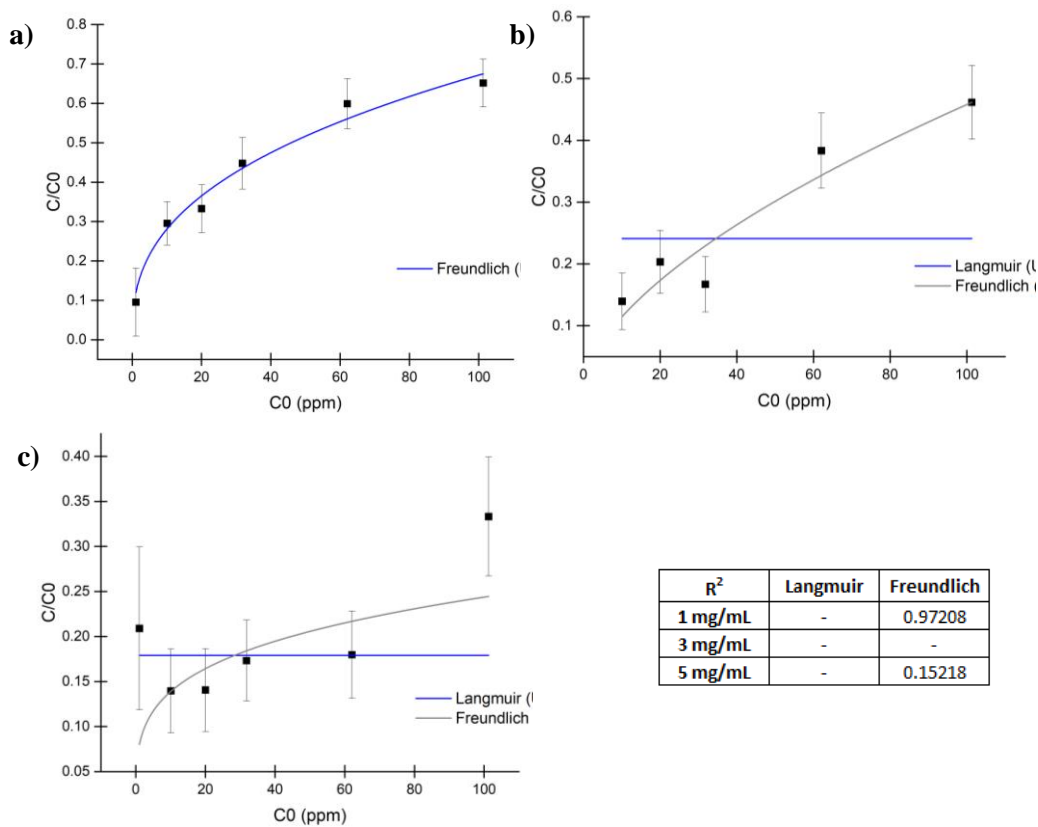


Figure 27. Curve fittings for material G with cellulose concentration of a) 1mg/mL b) 3 mg/mL and c) 5 mg/mL

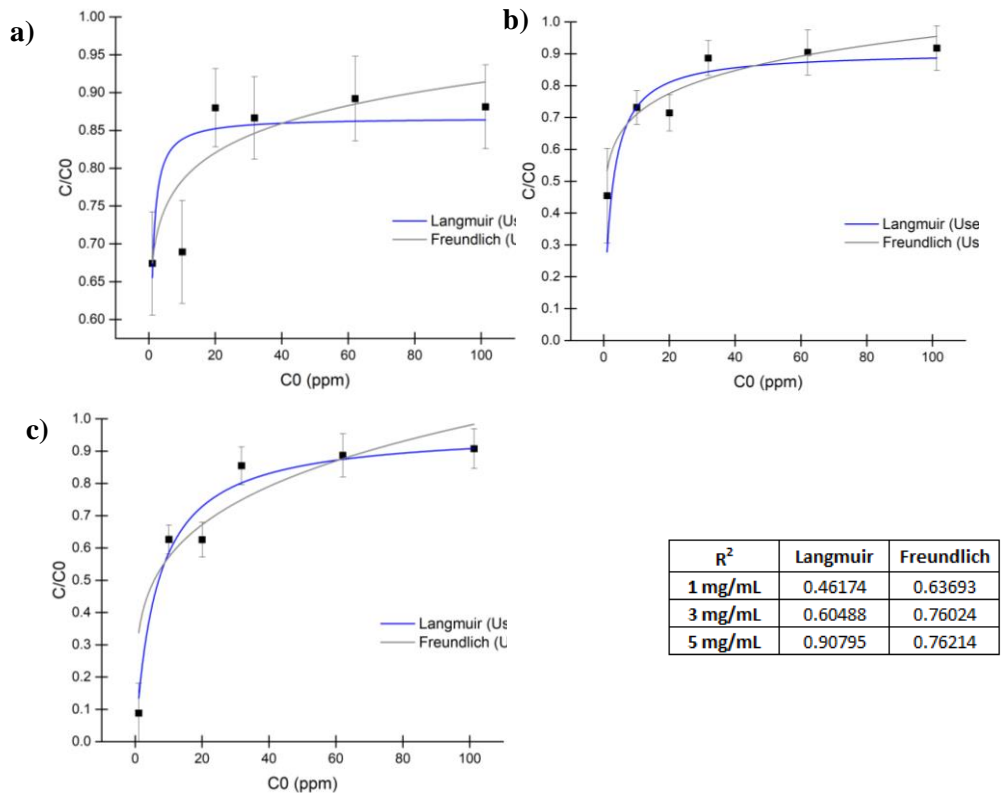


Figure 28. Curve fittings for material Af with cellulose concentration of a) 1mg/mL b) 3 mg/mL and c) 5 mg/mL

Lead essays

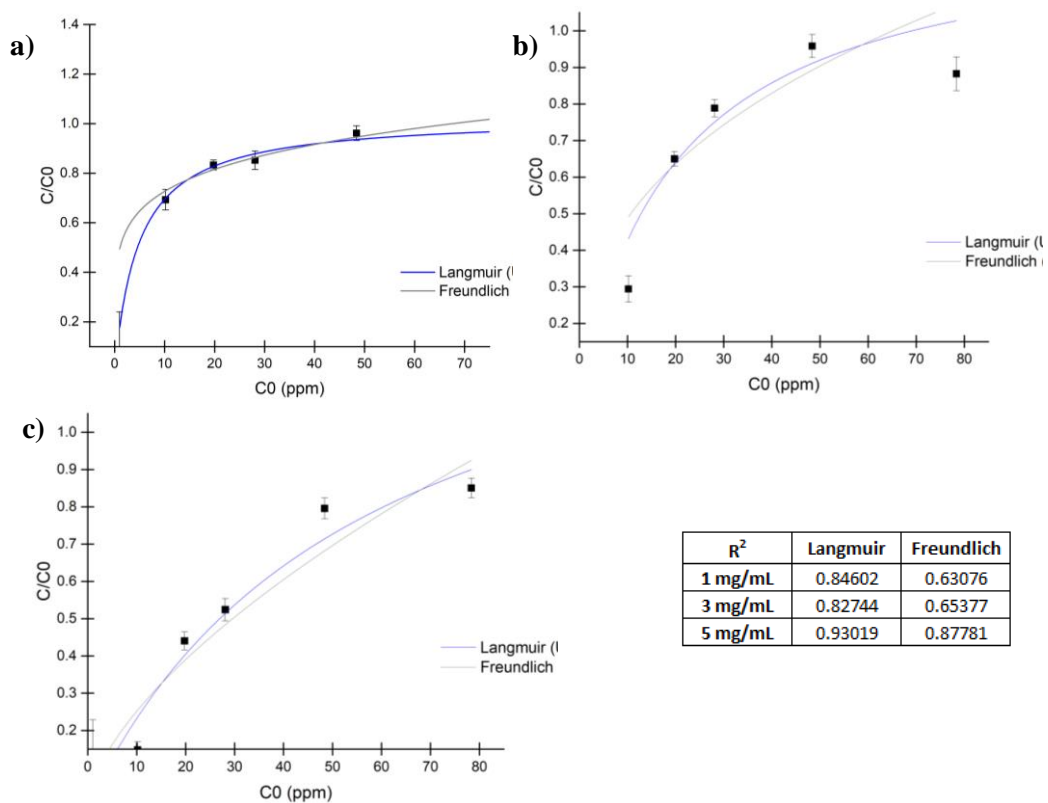


Figure 29. Curve fittings for material B1 with cellulose concentration of a) 1mg/mL b) 3 mg/mL and c) 5 mg/mL

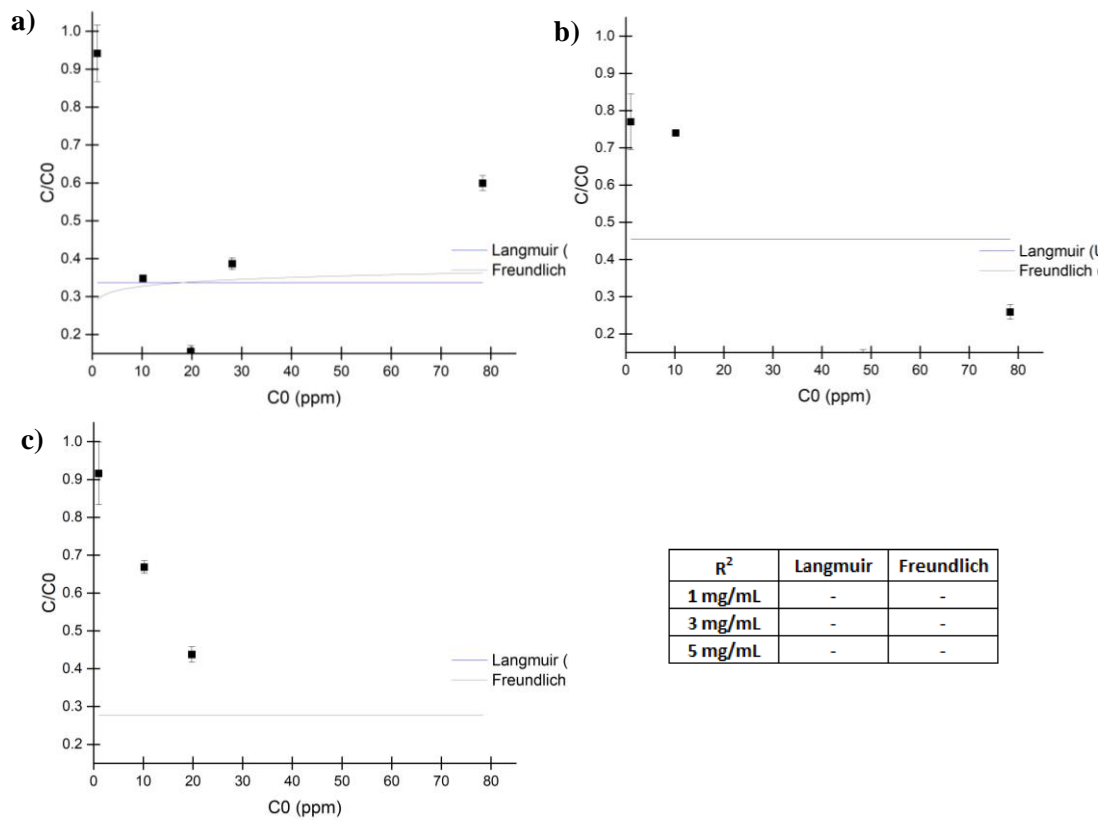


Figure 30. Curve fittings for material N2 with cellulose concentration of a) 1mg/mL b) 3 mg/mL and c) 5 mg/mL

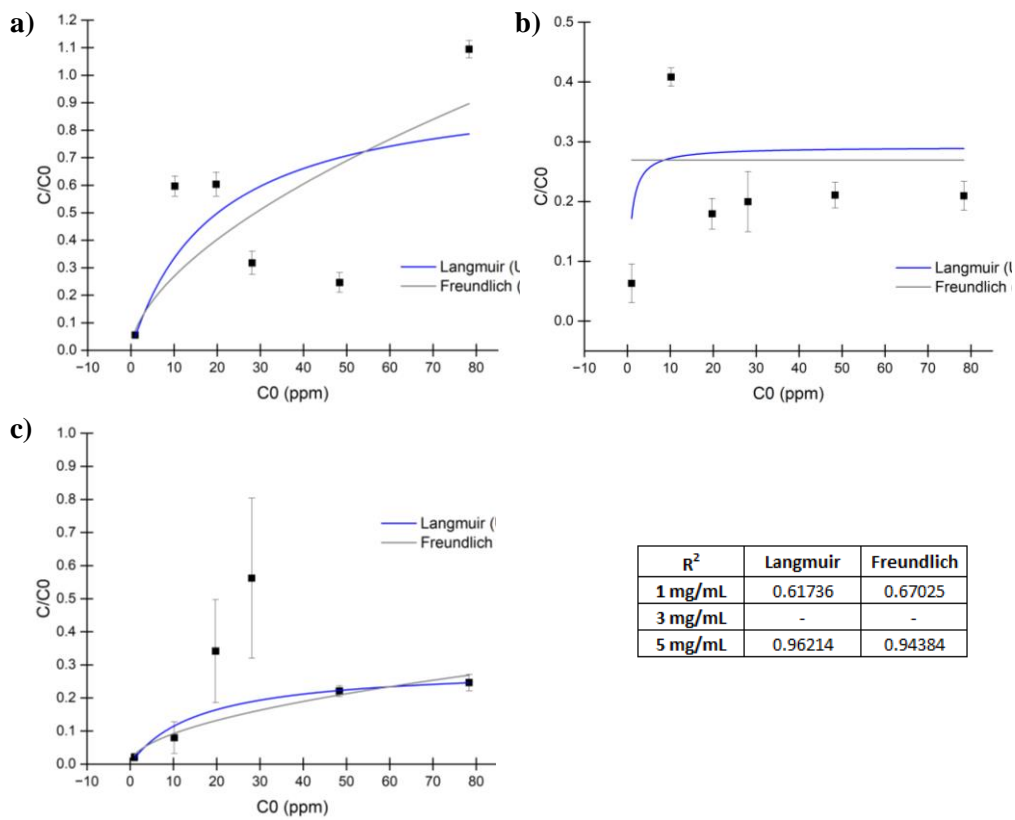


Figure 31. Curve fittings for material G with cellulose concentration of a) 1mg/mL b) 3 mg/mL and c) 5 mg/mL

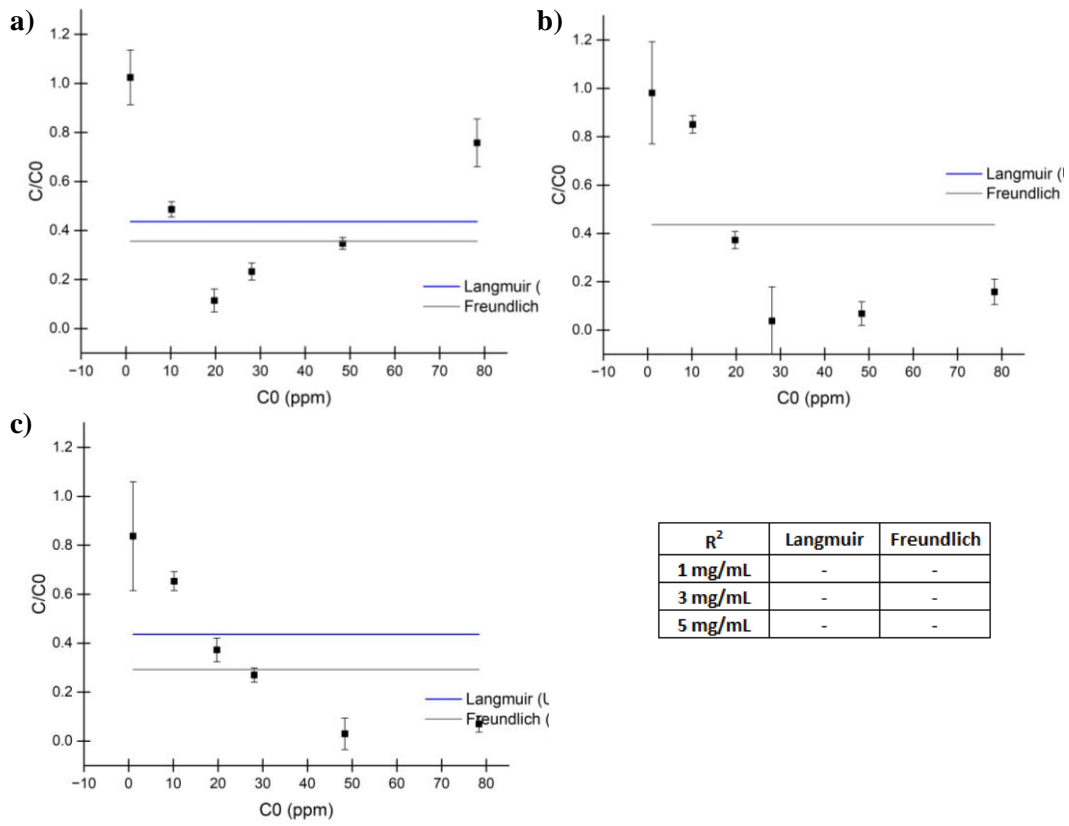


Figure 32. Curve fittings for material Ad with cellulose concentration of a) 1mg/mL b) 3 mg/mL and c) 5 mg/mL

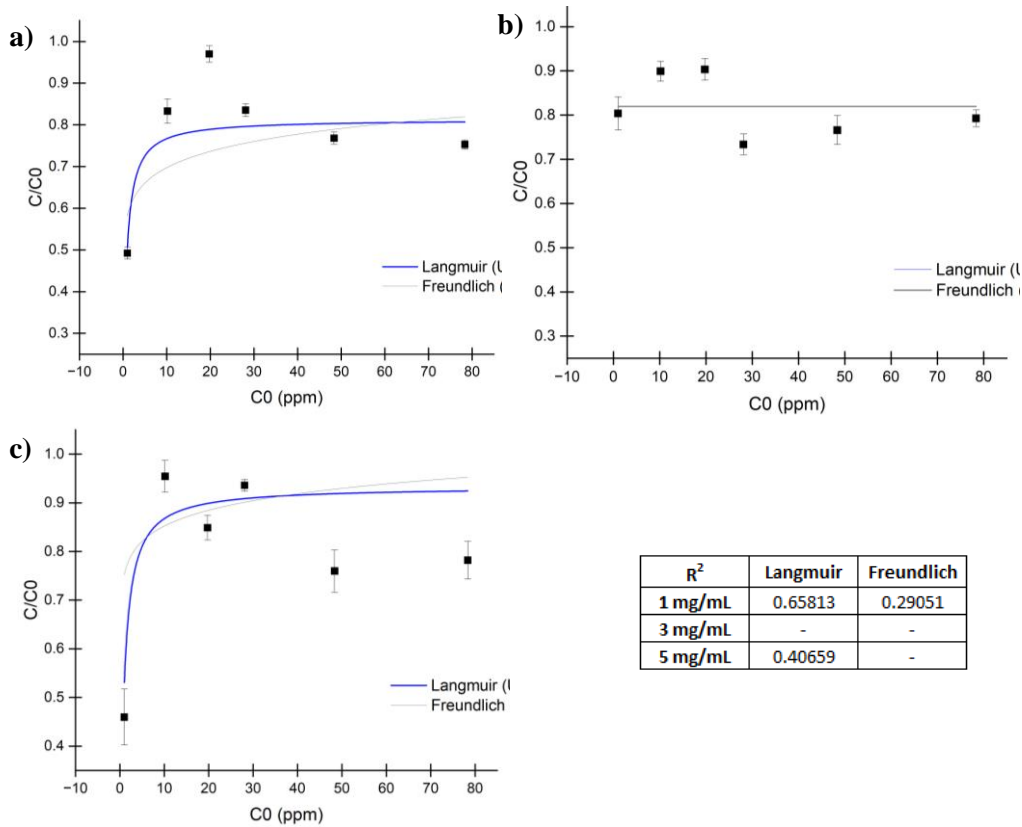


Figure 33. Curve fittings for material Af with cellulose concentration of a) 1mg/mL b) 3 mg/mL and c) 5 mg/mL

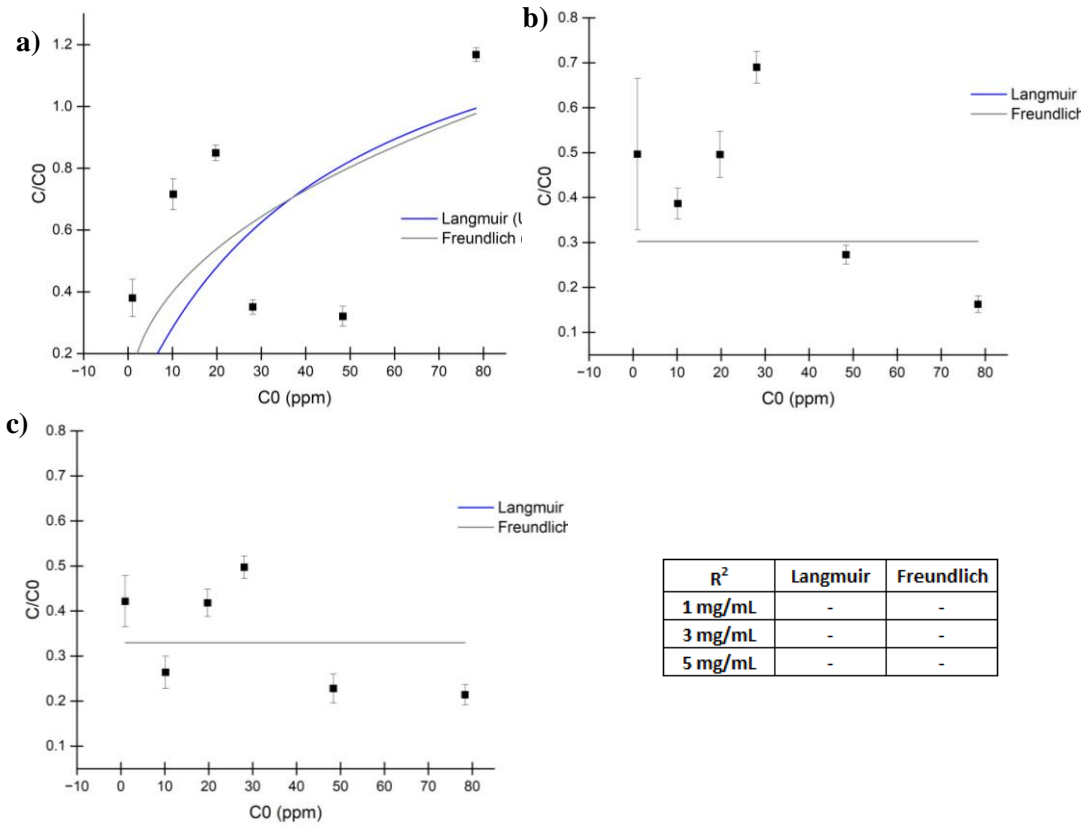


Figure 34. Curve fittings for material C with cellulose concentration of a) 1 mg/mL b) 3 mg/mL and c) 5 mg/mL

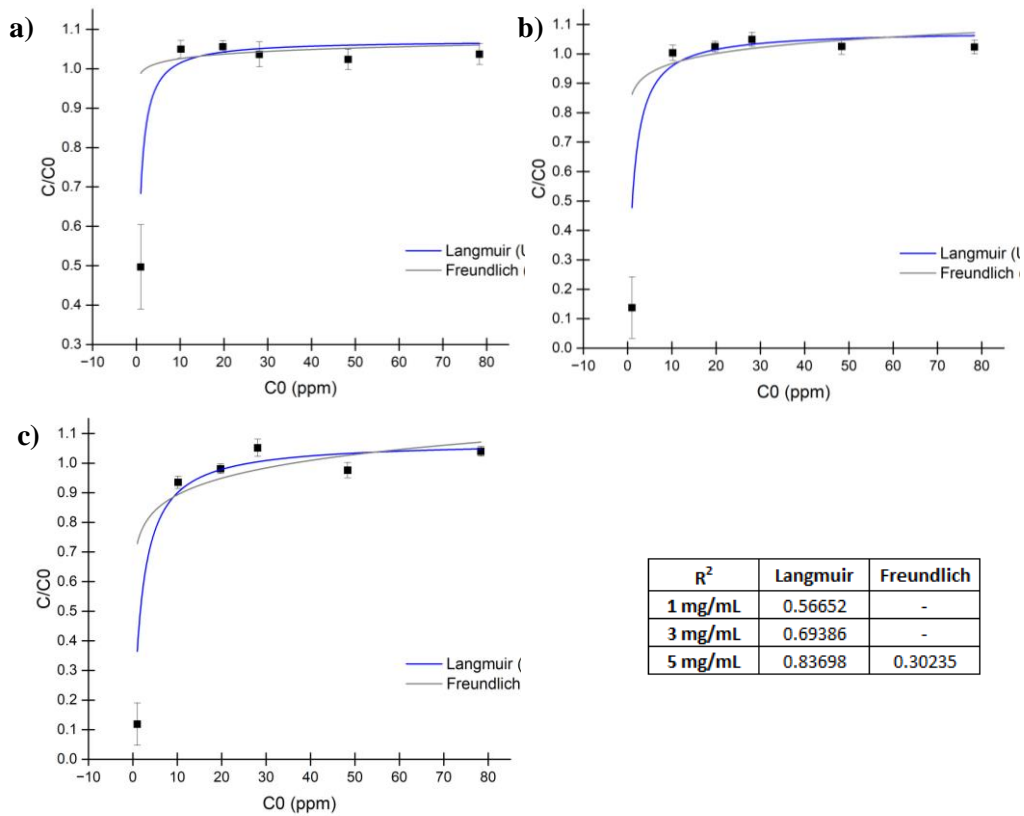


Figure 35. Curve fittings for material C1 with cellulose concentration of a) 1mg/mL b) 3 mg/mL and c) 5 mg/mL

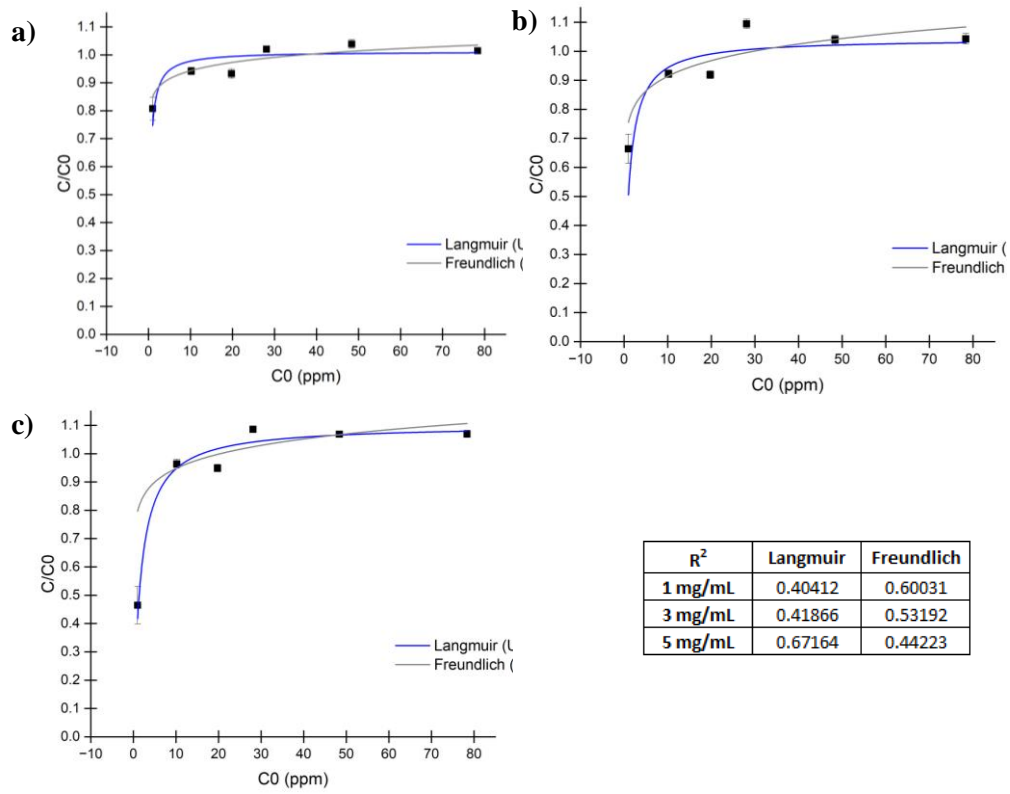


Figure 36. Curve fittings for material C4 with cellulose concentration of a) 1mg/mL b) 3 mg/mL and c) 5 mg/mL

Cadmium essays

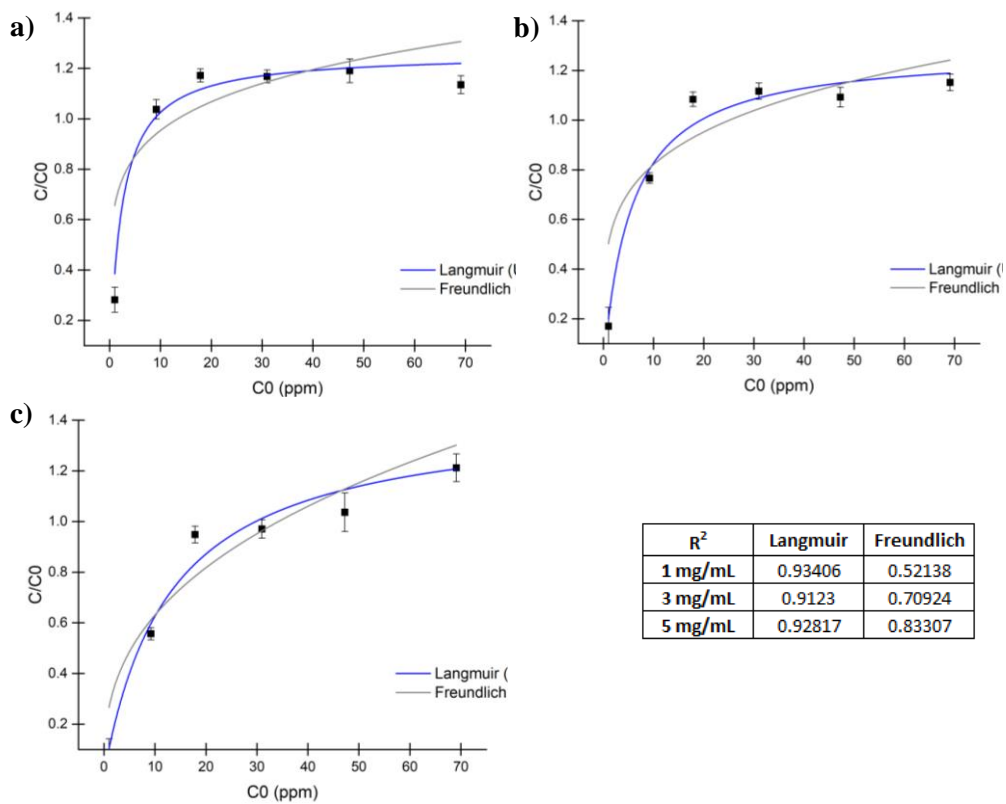


Figure 37. Curve fittings for material G with cellulose concentration of a) 1mg/mL b) 3 mg/mL and c) 5 mg/mL

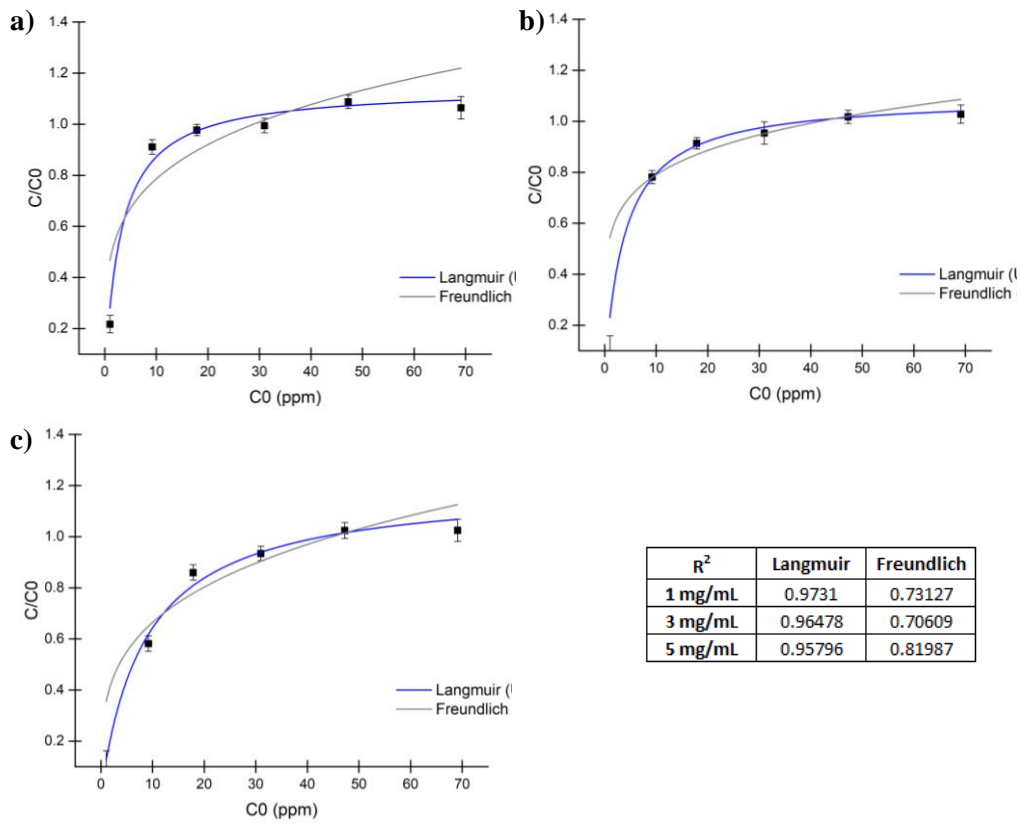


Figure 38. Curve fittings for material B1 with cellulose concentration of a) 1mg/mL b) 3 mg/mL and c) 5 mg/mL

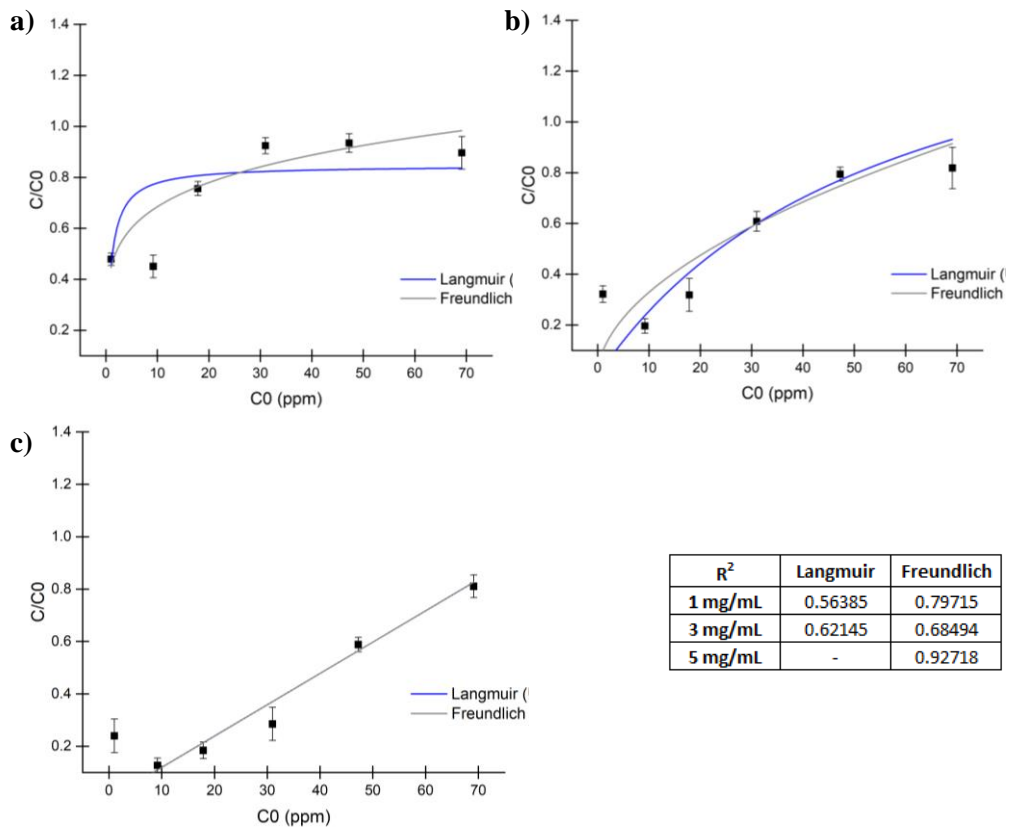


Figure 39. Curve fittings for material N2 with cellulose concentration of a) 1mg/mL b) 3 mg/mL and c) 5 mg/mL

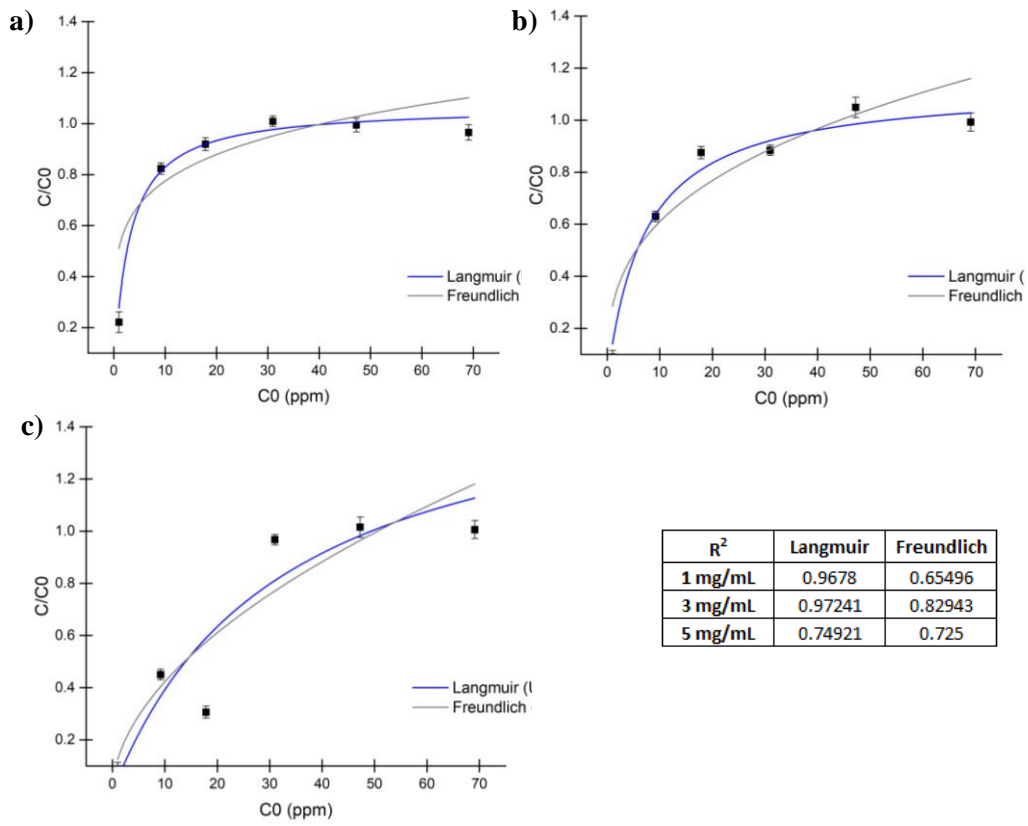


Figure 40. Curve fittings for material C with cellulose concentration of a) 1mg/mL b) 3 mg/mL and c) 5 mg/mL

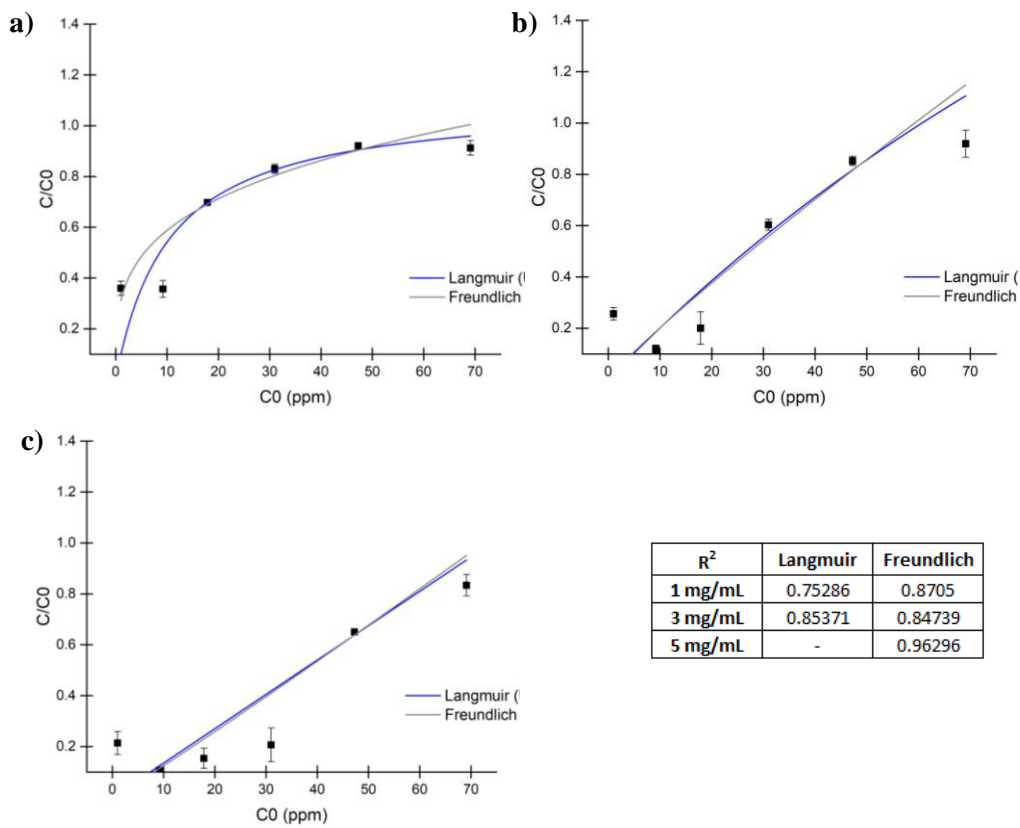


Figure 41. Curve fittings for material Ad with cellulose concentration of a) 1mg/mL b) 3 mg/mL and c) 5 mg/mL

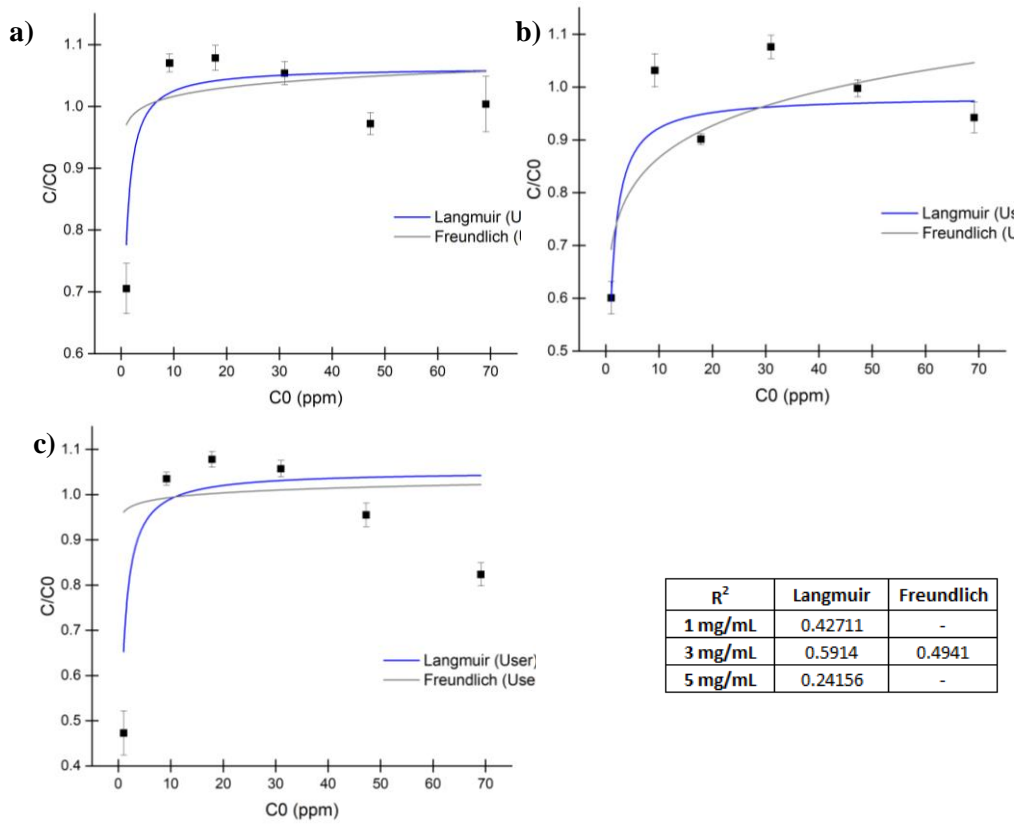


Figure 42. Curve fittings for material C1 with cellulose concentration of a) 1mg/mL b) 3 mg/mL and c) 5 mg/mL

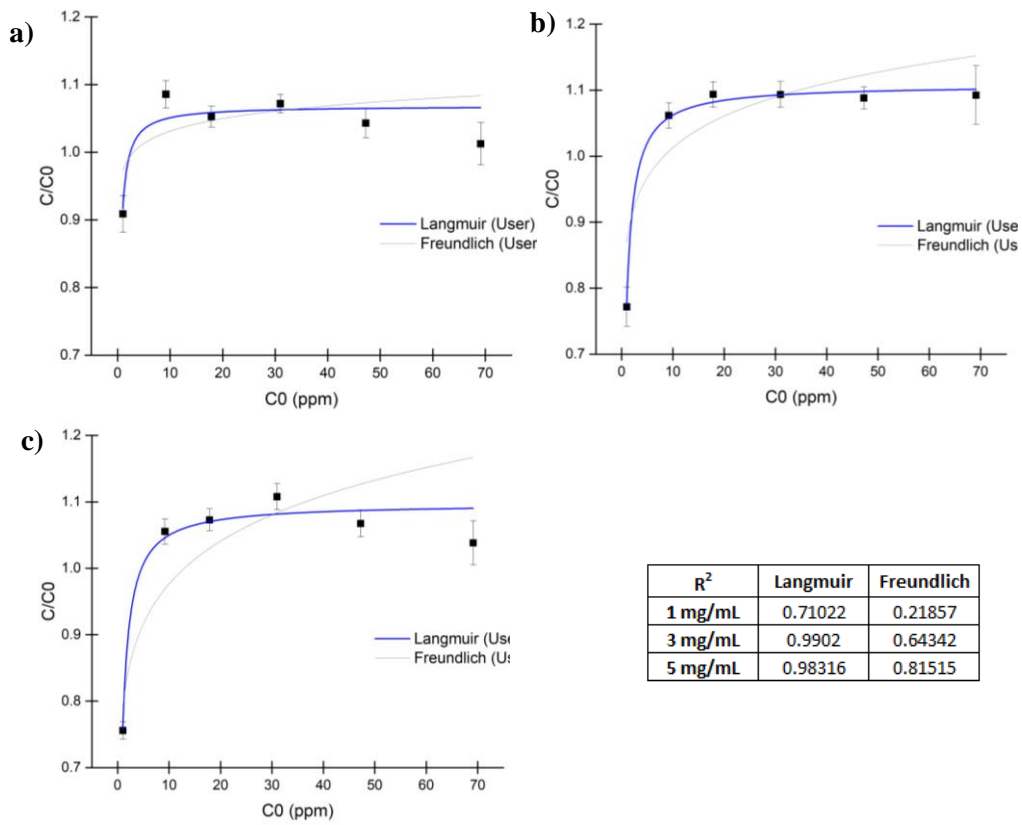


Figure 43. Curve fittings for material C4 with cellulose concentration of a) 1mg/mL b) 3 mg/mL and c) 5 mg/mL

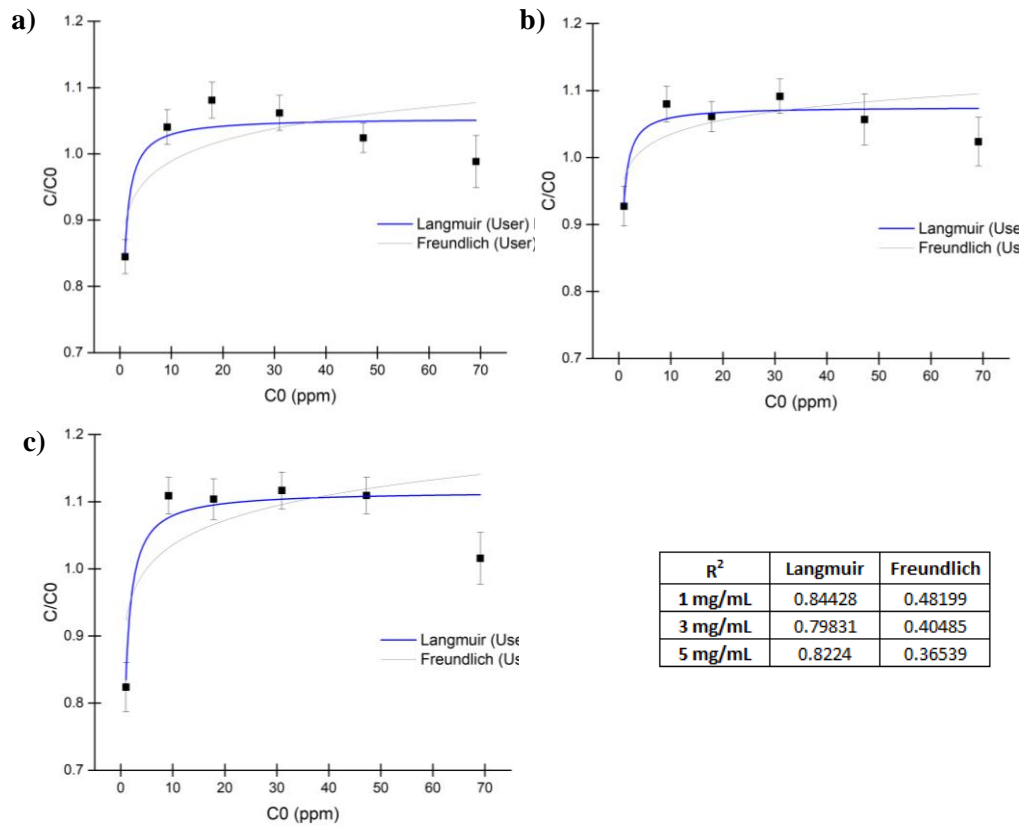


Figure 44. Curve fittings for material Af with cellulose concentration of a) 1mg/mL b) 3 mg/mL and c) 5 mg/mL

Annex D: Summary of Curve fittings to isotherm models

Table 8. Summary of curve fittings for copper data

Material	Material concentration	Langmuir model R ²	Freundlich model R ²	Best fit
C1	1 mg/mL	-	-	-
	3 mg/mL	0.34186	0.34444	0.34444
	5 mg/mL	0.57113	0.46275	0.57113
C4	1 mg/mL	0.68698	0.44903	0.68698
	3 mg/mL	0.99187	0.92572	0.99187
	5 mg/mL	0.94383	0.80761	0.94383
Af	1 mg/mL	0.46174	0.63693	0.63693
	3 mg/mL	0.60488	0.76024	0.76024
	5 mg/mL	0.90795	0.76214	0.90795
C	1 mg/mL	0.95478	0.81434	0.95478
	3 mg/mL	0.52573	0.68727	0.68727
	5 mg/mL	-	-	-
N2	1 mg/mL	-	-	-
	3 mg/mL	-	-	-
	5 mg/mL	-	0.92982	0.92982
Ad	1 mg/mL	-	-	-
	3 mg/mL	0.95479	0.73892	0.95479
	5 mg/mL	0.87872	0.89564	0.89564
G	1 mg/mL	-	0.97208	0.97208
	3 mg/mL	-	0.85325	0.85325
	5 mg/mL	-	-	-
B1	1 mg/mL	0.5064	0.54764	0.54764
	3 mg/mL	0.84528	0.84828	0.84828
	5 mg/mL	-	-	-

Table 9. Summary of curve fittings for lead data

Material	Material concentration	Langmuir model R²	Freundlich model R²	Best fit
C1	1 mg/mL	0.56652	-	0.56652
	3 mg/mL	0.69386	-	0.69386
	5 mg/mL	0.83698	0.30235	0.83698
C4	1 mg/mL	0.40412	0.60031	0.60031
	3 mg/mL	0.41866	0.53192	0.53192
	5 mg/mL	0.67164	0.44223	0.67164
Af	1 mg/mL	0.65813	0.29051	0.65813
	3 mg/mL	-	-	-
	5 mg/mL	0.40659	-	0.40659
C	1 mg/mL	-	-	-
	3 mg/mL	-	-	-
	5 mg/mL	-	-	-
N2	1 mg/mL	-	-	-
	3 mg/mL	-	-	-
	5 mg/mL	-	-	-
Ad	1 mg/mL	-	-	-
	3 mg/mL	-	-	-
	5 mg/mL	-	-	-
G	1 mg/mL	0.61736	0.67025	0.67025
	3 mg/mL	0.97844	0.88131	0.97844
	5 mg/mL	0.96214	0.94384	0.96214
B1	1 mg/mL	0.84602	0.63076	0.84602
	3 mg/mL	0.82744	0.65377	0.82744
	5 mg/mL	0.93019	0.87781	0.93019

Table 10. Summary of curve fittings for cadmium data

Material	Material concentration	Langmuir model R²	Freundlich model R²	Best fit
C1	1 mg/mL	0.42711	-	0.42711
	3 mg/mL	0.5914	0.4941	0.5914
	5 mg/mL	0.24156	-	0.24156
C4	1 mg/mL	0.71022	0.21857	0.71022
	3 mg/mL	0.9902	0.64342	0.9902
	5 mg/mL	0.98316	0.81515	0.98316
Af	1 mg/mL	0.84428	0.48199	0.84428
	3 mg/mL	0.79831	0.40485	0.79831
	5 mg/mL	0.8224	0.36539	0.8224
C	1 mg/mL	0.9678	0.65496	0.9678
	3 mg/mL	0.97241	0.82943	0.97241
	5 mg/mL	0.74921	0.725	0.74921
N2	1 mg/mL	0.56385	0.79715	0.79715
	3 mg/mL	0.62145	0.68494	0.68494
	5 mg/mL	-	0.92718	0.92718
Ad	1 mg/mL	0.75286	0.8705	0.8705
	3 mg/mL	0.85371	0.84739	0.85371
	5 mg/mL	-	0.96296	0.96296
G	1 mg/mL	0.93406	0.52138	0.93406
	3 mg/mL	0.9123	0.70924	0.9123
	5 mg/mL	0.92817	0.83307	0.92817
B1	1 mg/mL	0.9731	0.73127	0.9731
	3 mg/mL	0.96478	0.70609	0.96478
	5 mg/mL	0.95796	0.81987	0.95796